NASA
Technical
Paper
2377

August 1984

Development of In Situ Stiffness Properties for Shuttle Booster Filament Wound Case

V. Verderaime

NASA

NASA Technical Paper 2377

1984

Development of In Situ Stiffness Properties for Shuttle Booster Filament Wound Case

V. Verderaime

George C. Marshall Space Flight Center
Marshall Space Flight Center, Alabama

NASA

National Aeronautics and Space Administration

Scientific and Technical Information Branch

TABLE OF CONTENTS

LIST OF ILLUSTRATIONS

LIST OF TABLES

LIST OF SYMBOLS

A_{ij}	Extensional stiffness matrix components
C_{ij}	Lamina stiffness coefficients
D_{ij}	Bending stiffness matrix components
G_{ij}, g_n	Shear modulus and hydrotest characteristics
H	Hoop lamina thickness ratio
K	Arbitrary lamina layer
L, l	Shell length and growth, respectively
M	Moments and lamina property
N_x, N_θ	Force per unit length, axial and hoop
P	Hydroproof or combustion pressure
R	Shell inside radius
T, t	Thrust and laminate total thickness
V_f, V_m, V_d	Volume fraction of fiber, resin and voids
W_m	Resin weight ratio
α	Arbitrary lamina fiber orientation from X-axis
γ	Shear strain
δ	Variation
ϵ_x, ϵ_θ	Axial and hoop normal strains
ν_{12}, $\nu_{x\theta}$	Poisson's ratios, lamina and laminate
ξ	Halpin Tsai constants
ρ	Density
σ, τ	Normal and shear stress
m,n	Cos α and sin α, respectively
x,θ	Laminate axial and hoop directions

TECHNICAL PAPER

DEVELOPMENT OF IN-SITU STIFFNESS PROPERTIES FOR SHUTTLE BOOSTER FILAMENT WOUND CASE

I. INTRODUCTION

Recent experiences in formulating and producing appropriate shell stiffness properties for the graphite-epoxy wound motor case has necessitated an extension of prediction and verification methods over earlier practices. While neither theory nor fiber data was lacking at the inception of the Filament Wound Case (FWC) Project, the multitude of compelling structural requirements and the immense geometry of the article has rendered some engaging examples for discussion, enticement, and for more comprehensive planning on future applications.

The impetus for substituting filament wound case segments for the proven steel ones was the promise of graphite fibers' high specific strength and stiffness to reduce the vehicle weight such as to increase the payload delivered from the Western Test Range by 18 percent. Existing operational constraints were imposed and resulting technical challenges identified. The case segmentation was to comply with current casting, transportation and erection facilities, but no comparable jointed filament wound pressure vessel had been manufactured to provide the necessary confidence to commit the project. Of equal importance was the structural requirement that the Shuttle System's existing load limits were not to be exceeded, but, again, no comparable stiffness and dispersion data was available.

The Solid Rocket Booster Filament Wound Case (SRB FWC) program was preceded by two independent feasibility studies from February through October 1981. Studies concluded that a filament wound motor case should be a low technical and schedule risk program. It demonstrated through subscale model tests that a segmented FWC was highly feasible and it particularly disclosed the current understanding, methodology, and data base for coping with the structural stiffness requirements of the Shuttle systems loads. It was immediately perceived that this compliance depended primarily on developing an appropriate composite material data base and on developing a brief test program to achieve it. To this end, large bottle test specimens were negotiated for developing the A-basis allowables, which included extensional elastic constant determination, instead of the standard and more economical 6-in. bottle specimen. Sensitivity studies, statistical sampling test, subscale and component verification for math model updating were incorporated into the finally negotiated project to minimize major technical problems on the more time critical full-scale wound segments. The study could not dispel the suspicion of a scaling effect nor could those concerned communicate their concerns – scaling what and why? That was a bridge to come.

The FWC development has certainly contended with its share of problems, including the in-situ membrane response, which almost deluded many participating composite analysts. The extent of this learning was demonstrated by the many significant baseline changes of the composite design. What began as a material compliance devoid of new concepts and fundamental insights, each new graphite bottle design and hydrotest uncovered mistaken computations and stiffness math modeling which persisted during most of the development phase. It was not until the third quarter-scale hydro and dynamics tests, when results were diligently examined and compared, that the unpredictable responses suggested to the author a new awareness of essential phenomena that lead to discovering unexpected parameters which significantly modified the data analysis method and modeling techniques.

Results presented in this paper are by no means conclusive but are intended to initiate a probe to force a solution into this obscure phenomena of filament wound composites which is quite apart from the extensive application of graphite cloth. All data and techniques used by the author are presented in the hope that others inclined to hack at this elastic code may circumvent any prejudices and perhaps misguided intuitions incorporated into preliminary conclusions. Final conclusions will have to wait until the bulk of flight-type specimen are manufactured and hydro-proofed.

At this writing, only one flight-type, full-scale FWC segment has been tested. It represents the largest jointed, graphite-epoxy vessel ever built to operate with an internal pressure of 1000 psi. A more striking distinction will be achieved when the FWC segments are man-rated. Nevertheless, a number of prescriptions for the general development achievements of the elastic compliance are clearly evident. First and foremost was the indepth knowledge of composite mechanics, the fabrication experience and mastery of instrumentation and meaningful testing demonstrated by the manufacturer through numerous reports, reviews, and discussions. Of equal importance is that dynamicists were engaged in the composite description and elastic characteristics from the outset of the feasibility study. It follows that as the specific strength of large elastic structures increases, the elastic potential energy becomes more critical and the loads and dynamicist role more prominent. That role becomes eminent in all phases of design, development and changes when structural material is anisotropic. Finally, early Technical Interchange Meetings with associated contractors and centers were indispensible for the performance deficiencies revealed that were more suitably assessed and resolved by the affected users.

Special recognition is here due Dr. George McDonough for staffing this effort and for his encouragement during real time data flow and respective events that led to new basic conclusions that might otherwise have been lost to investigators. The author further acknowledges data and reports generated by W. Hill, J. York, J. Schutz and C. Kirchner from Hercules, Inc. that were ultimately constructed into Tables 1, 3, 5, 6, 7, 8, and 9.

II. FILAMENT WOUND CASE CONFIGURATION

The solid rocket motor case of the Space Shuttle is segmented to simplify handling, shipping, and propellant grain casting. The four filament wound cylindrical segments shown in Figure 1 are field-spliced

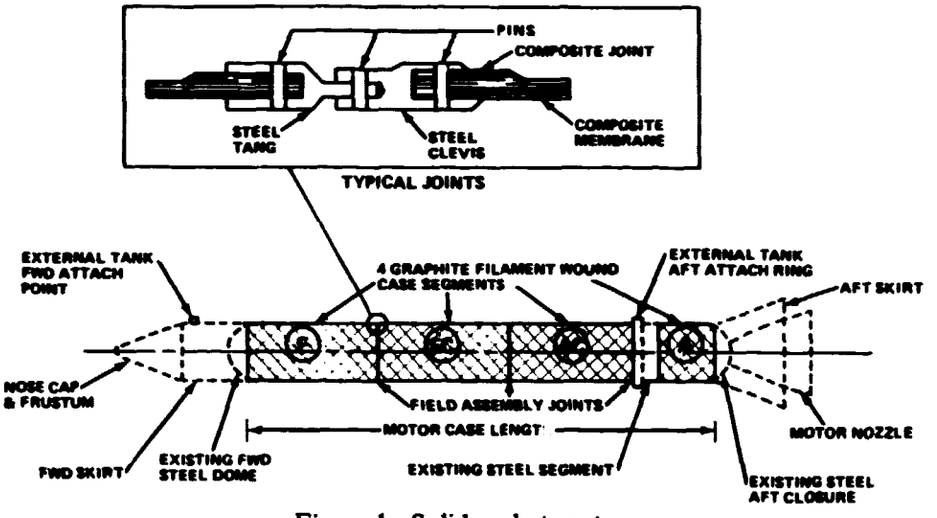

Figure 1. Solid rocket motor.

by pinning the steel tang and clevis rings as illustrated. Steel-to-steel joints are essentially identical to the existing steel motor case and are interchangeable. The composite cylinder ends are joined to the steel rings by a similarly pinned tang and clevis arrangement. The length of these segments is defined by field splice stations which are common to the steel motor case field joints. The two end domes and external tank attach segment are the existing steel configurations and are applicable to either steel or FWC segments. Because the FWC and existing steel motor case must be interchanged on the Solid Rocket Booster and must interface with existing Shuttle elements and launch facilities, the end result is that seven steel case segments are replaced by four composite segments.

The composite shell is manufactured from graphite fibers wetted with epoxy and wound on an aluminum mandrel in layers. Each layer thickness and fiber direction varies by design to satisfy membrane stiffnesses and joint integrity. The membrane construction is dominant and consists of alternating hoop and balanced helical laminae. The layup is essentially symmetrical with the mid-thickness which avoids coupling between extensional and bending deformation so that the matrix $B_{ij} = 0$ forms a more efficient structure. The joint ends were thickened with interspersed layers of axially oriented fiber to reduce pin-hole bearing stresses and local deformation. Each case segment is then cured at 390°F through a specified schedule. The inner surface is ultimately insulated with a rubber coating and cured at 290°F before casting the propellant grain.

III. COMPOSITE STIFFNESS REQUIREMENTS

Each FWC segment represents an orthotropic cylindrical shell that was optimized for structural strength and stiffness with weight. The shell is essentially subjected to in-plane loading (Fig. 2) so that the classical laminate plate theory [1] is a convenient basis for defining the symmetrical (or specially orthotropic) element response in the form

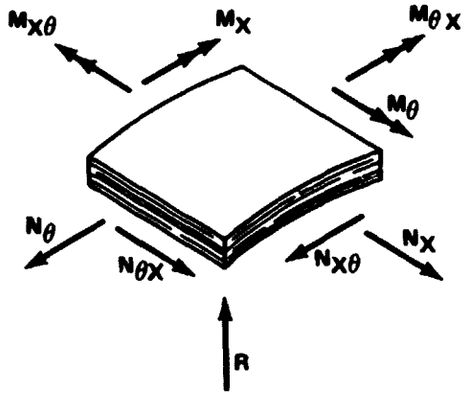

Figure 2. Membrane element.

$$\begin{Bmatrix} N_X \\ N_\theta \\ N_{X\theta} \end{Bmatrix} = \begin{bmatrix} A_{11} & A_{12} & 0 \\ & A_{22} & 0 \\ & & A_{66} \end{bmatrix} \begin{Bmatrix} \epsilon_X \\ \epsilon_\theta \\ \gamma_{X\theta} \end{Bmatrix} \quad (1)$$

for extensional and

$$\begin{Bmatrix} M_X \\ M_\theta \\ M_{X\theta} \end{Bmatrix} = \begin{bmatrix} D_{11} & D_{12} & 0 \\ & D_{22} & 0 \\ & & D_{66} \end{bmatrix} \begin{Bmatrix} k_X \\ k_\theta \\ k_{X\theta} \end{Bmatrix} \quad (2)$$

for bending deformations. Consequently, all stiffness constraints and requirements imposed on the FWC performance were manifested by the A_{ij} and D_{ij} matrices which follow.

a) Axial Growth Rate is a critical stiffness constraint during thrust buildup because it excites structural components attached forward of the solid rocket booster, the external tank lox dome in particular. The thrust buildup rate was fixed so that the axial excursion between the forward and aft skirts was limited to 0.6 in. when subjected to combustion pressure of 1004 psig and 3.35M lb thrust. When the elongation resulting from joint tolerances and deformation was deducted, the elongation budgeted to the membrane was expressed by

$$\ell = L\,\epsilon_x = \frac{L}{t}\left[\frac{N_x}{E_x} - \nu_{\theta x}\frac{N_\theta}{E_\theta}\right] \tag{3}$$

where

$$N_x = P\frac{R}{2} - \frac{T}{2\pi R} \qquad \text{and} \qquad N_\theta = PR$$

Since the case envelope and loads were constrained by existing Shuttle interfaces, the only opened parameters were the composite thickness and engineering elastic constants. When these were translated into matrix components of equation (1) by the relationships

$$\frac{1}{E_x t} = \frac{A_{22}}{A_{11}A_{22} - A_{12}^2} \qquad \frac{1}{E_\theta t} = \frac{A_{11}}{A_{11}A_{22} - A_{12}^2}$$

$$\frac{\nu_{\theta x}}{E_\theta t} = \frac{\nu_{x\theta}}{E_x t} = \frac{A_{12}}{A_{11}A_{22} - A_{12}^2} \quad , \quad \nu_{x\theta} = \frac{A_{12}}{A_{22}}$$

the elongation requirement was appropriately rewritten as

$$\ell = L\,\epsilon_x = L\left[\frac{N_x A_{22} - N_\theta A_{12}}{A_{11}A_{22} - A_{12}^2}\right] \tag{4}$$

b) Bending Axial stiffness was also specified to avoid the FWC fundamental frequencies from coupling with the vehicle control system frequencies of approximately 0.2 Hz. This stiffness was defined as the product of laminate variables

$$E_x t \geq 10^7 \text{ lbs/in.}$$

or

$$[A_{11}A_{22} - A_{12}^2]/A_{22} \geq 10^7 \quad . \tag{5}$$

c) Radial Growth of the forward segment was restricted to not exceed the propellant grain tangential strain capability and was specified by

$$\Delta R = R\,\epsilon_\theta = \frac{R}{t}\left[\frac{N_\theta}{E_\theta} - \nu_{x\theta}\frac{N_x}{E_x}\right]$$

or (6)

$$R\left[\frac{N_\theta A_{11} - N_x A_{12}}{A_{11}A_{22} - A_{12}^2}\right] \leq 0.58 \text{ in.}$$

d) Structural Integrity of the membrane also implied a stiffness constraint. The tangential unit load was much larger than the axial unit load, equations (3), so that the hoop fiber ultimate strain was related to the hoop fiber ultimate stress,

$$\sigma_{f_{ult.}} = E_{f_L}\epsilon_{f_{ult.}}$$

or (7)

$$\sigma_{f_{ult.}} = E_{f_L}\left[\frac{N_\theta A_{11} - N_x A_{12}}{A_{11}A_{22} - A_{12}^2}\right]_{ULT.}$$

because the hoop fiber strain is identically equal to the laminate tangential strain.

e) The only requirement imposed on the bending stiffness matrix was that the D_{ij} components be defined within the accuracy essential for modal analysis to support dynamics response studies and for buckling analysis to sustain water impact loads.

Having implicitly related the laminate properties to constraints by the above equations, the design challenge was to satisfy them all with minimum structural weight through material selections, winding geometries and controlled processing. The intermediate graphite fiber was selected because of its high specific strength and modulus, and its available data base along with economic considerations. The only structural requirement on the epoxy was its ability to bind the fibers together and effectively distribute the multi-axial loads. The primary criteria was therefore to select an epoxy that was compatible with manufacturing processes, handling, and operational environments. Performance wise, the lowest epoxy to fiber mix ratio contributed the highest specific strength and stiffness in the fiber direction.

Satisfying the FWC requirements through winding geometries was not so obvious and demands a brief review of all winding parameters available to the laminate designer and will be covered in Section IV. Even less obvious were the processing controls and independent parameters affecting the lamina which makeup the laminate and was the subject of this investigation.

IV. LAMINATE DESIGN PARAMETERS

Adjacent layers having common winding angles are identified as a lamina having orthotropic properties with respect to its principal axes (Fig. 3), and are translatable to another set of axes such as the cylindrical axes. Because the wound lamina transverse properties in the 2-direction are equal to those in the 3-direction, it is further classified as transversally orthotropic and the stress strain relationship,

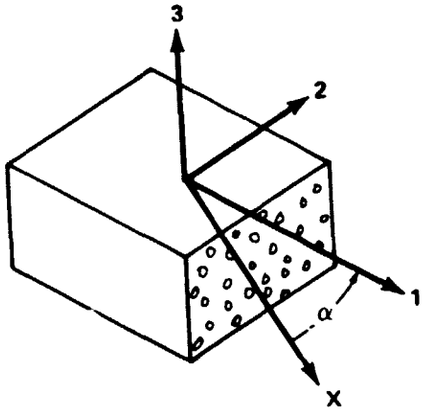

Figure 3. Wound lamina coordinates.

$$\sigma_i = [C_{ij}]\ \epsilon_j$$

is characterized by a total of five elastic constants which are related to engineering constants as follows:

$$C_{11} = \frac{E_1^2}{E_1 - E_2 \nu_{12}^2}$$

$$C_{22} = \frac{E_2 E_1}{E_1 - E_2 \nu_{12}^2} \quad , \quad C_{12} = \nu_{12} C_{22} \quad , \quad C_{44} = C_{23} = \frac{E_2}{2(1+\nu_{23})} \tag{8}$$

$$C_{55} = C_{66} = G_{12} \quad , \quad C_{23} = C_{22} - 2C_{44}$$

All other matrix components are either symmetrical or zero.

The FWC is plied in the hoop lamina with the fiber 1-direction oriented at $\alpha = 90$ deg from the cylinder x-axis and the balanced helical laminae are oriented at some specified $+\alpha$ and $-\alpha$ angles. Sum of all hoop lamina thickness to total laminate thickness,

$$H = \frac{\sum \text{hoop thickness}}{\text{Laminate thickness}} \tag{9}$$

is a useful design index if all hoop lamina properties are identical, otherwise, a modified ratio is necessary.

To correlate the hoop and helical lamina properties to a common axis, cylinder x-axis, a fourth order transformation is used with equations (8) to give the transformed reduced stiffness:

$$\bar{C}_{11} = C_{11} m^4 + 2(C_{12} + 2C_{66}) m^2 n^2 + C_{22} n^4$$

$$\bar{C}_{12} = (C_{11} + C_{22} - 4C_{66}) m^2 n^2 + C_{12} (m^4 + n^4) \tag{10}$$

$$\bar{C}_{22} = C_{11}\, n^4 + 2(C_{12} + 2C_{66})m^2 n^2 + C_{22}\, m^4$$

$$\bar{C}_{66} = (C_{11} + C_{22} - 2C_{12} - 2C_{66})m^2 n^2 + C_{66}\,(m^4 + n^4)$$

$$\bar{C}_{16} = (C_{11} - C_{12} - 2C_{66})m^3 n + (C_{12} - C_{22} + 2C_{66})m\, n^3$$

$$\bar{C}_{26} = (C_{11} - C_{12} - 2C_{66})\, m\, n^3 + (C_{12} - C_{22} + 2C_{66})m^3 n \qquad (10)$$

(Cont.)

$$\bar{C}_{23} = C_{12}\, n^2 + C_{23}\, m^2$$

$$\bar{C}_{44} = C_{44}\, m^2 + C_{55}\, n^2$$

$$\bar{C}_{55} = C_{44}\, n^2 + C_{55}\, m^2 \quad ,$$

where $m = \cos\alpha$ and $n = \sin\alpha$.

Integrating these hoop and helical plied laminae properties over the laminate thickness in accordance with Figure 4,

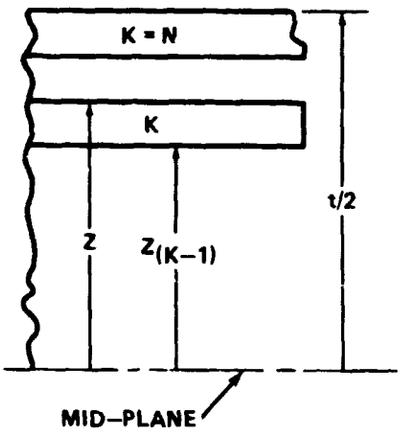

Figure 4. N-plied laminate about mid-plane.

$$A_{ij} = \sum_{k=1}^{N} (\bar{C}_{ij})_k \,[z_k - z_{(K-1)}]$$

$$D_{ij} = \sum_{k=1}^{N} (\bar{C}_{ij})_k \,[z_k^3 - Z_{(k-1)}^3] \quad , \qquad (11)$$

results into the laminate stiffness components where A_{11} and A_{22} are in the cylinder x and θ axes to conform with constraint equations (4), (5), (6), and (7).

Note that the laminate stiffnesses of equation (11) incorporate only three independent variables, α, H and t If the designer increases the thickness to satisfy the constraint equations of Section III, he will violate the minimum weight requirement. If he increases the wrap angle or the hoop ratio, he satisfies the axial growth and bending stiffness but encroaches on the grain and case integrity (Fig. 5). An optimization was indicated during the feasibility study, but until the stiffness property dispersions were developed, margins could not be realistically assigned to these constraints.

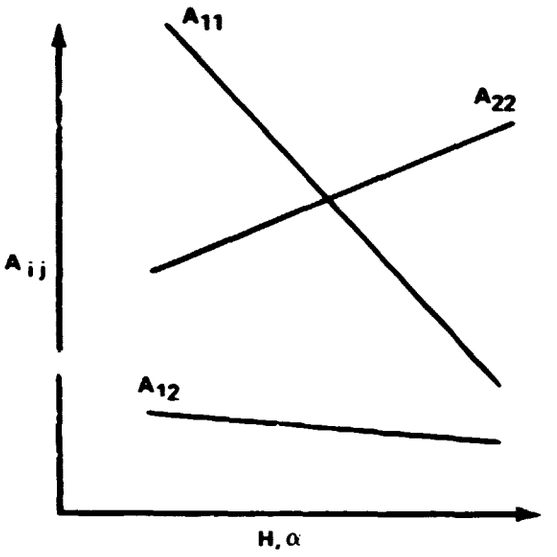

Figure 5. Stiffness sensitivities.

A minor infringement on optimum design was that all segments were specified to have a common helical angle and hoop ratio so that a single composite system with "A-basis" properties and dispersion need be developed. The variation of combustion pressure and external loads acting along the total length of the FWC were satisfied by varying segment laminate thickness. The resulting weight increase was not significant compared to the benefits of cost and schedules.

V. LAMINA PRELIMINARY MODEL

Given that the fiber, resin and mix have been ideally selected, how might they be modeled to reproduce an experimentally derived lamina elastic response was the next consideration. The Halpin-Tsai [2] model is extensively used and was favored for this study. The Halpin-Tsai equations not only contain parameters that may be adjusted for manufacturing variations, but they reduce the more rigorous model to an approximate form consisting of

$$M = \frac{M_f (1 + \xi V_f) + M_m \xi (1 - V_f)}{(1 - V_f) M_f/M_m + \xi + V_f} \tag{12}$$

to bound the lower limit properties and the rule of mixtures

$$M = M_f V_f + M_m (1 - V_f) \tag{13}$$

to bound the upper limit properties when the constant $\xi \to \infty$. M symbolizes the elastic property to be determined and the known input fiber and matrix (resin) properties are respectively subscripted. Because the Halpin-Tsai constant, ξ, was experimentally derived for each new lamina system, it also compensated for ineptly defined constituent properties. This feature was exploited in defining the HBRF-55A resin

input properties. Over a dozen neat resin samples were cured, post-cured, and uniaxially tested. The tensile modulus spread was between 0.36 and 0.60 Msi and a mean of E_m = 0.49 Msi was estimated for the model. Other neat resin properties were also estimated because the real strain state was uncertain and the model was conveniently forgiving.

The AS4W-12K graphite fiber properties measured from each lot are listed in Table 1. Orthotropic properties of the fiber were estimated from References 4 through 7 for carbon filament (less than 3000°F exposure) and noted in Table 2.

TABLE 1. FIBER LOT PROPERTIES AS4W - 12K GRAPHITE

Lot No.	Modulus MSI		ρ_f lb/in.^{3}	Area per tow 10^{-4} in.^{2}
	E_{f_l}	Secant		
607-3I	33.5	35	0.0657	7.321
607-3J	33	34	0.0654	7.358
607-3N	35	36.7	0.0646	7.551
607-3P	34	35.8	0.0648	7.315
616-4F	33	34	0.0648	7.054
617-4F	33	34.1	0.0652	7.066
617-4G	33	34.7	0.0649	7.105
618-3C	33	34.7	0.0647	7.397
619-3A	34	35.3	0.0642	7.530
621-3A	34	34.9	0.0654	7.037
629-3C	34	34.5	0.0652	7.101
630-3A	34	35.9	0.0653	7.049
632-4B	33	35.5	0.0649	7.435
634-4F	34	35	0.0644	7.547
634-4G	34	35.3	0.0644	7.564
640-4B	32.6	34	0.0646	7.385

TABLE 2. ASSUMED CARBON FILAMENT PROPERTIES

Symbol	Orthotropic Properties	Nominal
E_{f_T}	Transverse Young Modulus, Msi	2.2
$G_{f_{LT}}$	Transverse Shear Modulus, Msi	3.3
ν_{f_L}	Longitudinal Poission's Ratio	0.29

To model the series connected constituents, equation (12), a series of simulated lamina tubes were tested to determine the Halpin-Tsai constant. Cylinders 4-in. in diameter were wound in hoop only and then cured and post cured. Forty-eight specimens were cut to 3-in. lengths and each was first tested in torsion well below the ultimate and then stressed in tension until failure. Results are summarized in Table 3.

TABLE 3. LAMINA TUBE TEST RESULTS [3]

Symbol	Lamina Properties	Nominal	Percent C.V.
G_{12}	Inplane Torsion Modulus, Msi	0.64	10
E_2	Transverse Modulus, Msi	0.99	9
ϵ_{2ULT}	Ultimate Transverse Strain, percent	0.293	–
V_f	Fiber Volume, percent	51.2	–
V_d	Void Volume, percent	5.9	–

The resin modulii were degraded for voids.

$$E'_m = E_m (1 - V_d)$$

$$G_m = E'_m/2 (1 - \nu_m) \qquad (14)$$

and substituted into the rearranged equation (12)

$$\xi = \frac{M[(1 - V_f) M_f/M_m + V_f] - M_f}{M_m - M + V_f (M_f - M_m)} \qquad (15)$$

Transverse properties (Table 2) and 4-in. tube lamina test results (Table 3) were used with equation (15) to obtain the Halpin-Tsai constants for the epoxy dominated lamina modulii:

Young Transverse, $\xi_E = 1.7$

In-Plane Shear, $\xi_G = 2.7$ (16)

The lamina modulus in the fiber direction and the major Poisson's ratio are parallel connected mixtures and comply with the rule of mixtures, equation (13). Correction for void content is unnecessary because it is offset by the multi-strain state of the resin. The lamina preliminary stiffness characteristics were accordingly modeled by

$$E_1 = E_{f_L} V_f + E_m (1 - V_f)$$

$$\nu_{12} = 0.29 V_f + 0.35 (1 - V_f)$$

$$E_2 = \frac{E_{f_T} (1 + 1.7 V_f) + E'_m 1.7 (1 - V_f)}{(1 - V_f) E_{f_T}/E'_m + 1.7 + V_f} \qquad (17)$$

$$G_{12} = \frac{G_{f_{LT}} (1 + 2.7 V_f) + G_m 2.7 (1 - V_f)}{(1 - V_f) G_{f_{LT}}/G_m + 2.7 + V_f}$$

Selected design conditions of

$$V_f = 0.55 \quad , \quad V_d = 0.05 \quad , \quad E_{f_L} = 33.4 \text{ Msi} \quad ,$$

were incorporated to predict the FWC lamina elastic properties (Table 4).

TABLE 4. LAMINA PRELIMINARY PROPERTIES

Symbol	Lamina Design Properties	Nominal
E_1	Longitudinal Modulus, Msi	18.6
E_2	Transverse Modulus, Msi	1.0
G_{12}	Shear Modulus, Msi	0.7
ν_{12}	Poisson's Ratio	0.3

Before winding, the mandrel is covered with a 0.02-in. thick graphite cloth to provide a smooth interface and serve as an inner surface protective structure during the insulation coating process. A similar surface is provided on quarter scale articles by a 0.02-in. thick glass cloth to scale down its contribution to the total stiffness. In each case, the cloth is assumed to act as a lamina 0.01-in. thick in the woof direction and 0.01-in. lamina in the warp direction. Respective laminae properties are listed in Table 5.

TABLE 5. CLOTH LAMINA PROPERTIES

Symbol	Elastic Properties	Glass	Graphite
E_1	Longitudinal Modulus, Msi	6.6	17.4
E_2	Transverse Modulus, Msi	2.0	1.6
G_{12}	Shear Modulus, Msi	0.76	0.71
ν_{12}	Poisson's Ratio	0.28	0.28

VI. LAMINATE PERFORMANCE TESTS

As is frequently the case, developing experimental evidence to verify design predictions is the most technically exacting and programmatically demanding phase of many high performance projects. Testing tasks are further compounded when a statistical basis is imposed on subscale specimen.

In reviewing constraint equations (5) through (7), it was noted that all but one could be directly verified by measuring the axial and hoop strains during hydrotest. It was then believed that since the most common procedure for establishing the A-basis strength of a laminate system was to hydroburst numerous 6-in. bottles, appropriate instrumentation might ride on larger bottles to back out, statistically [8] the most significant elastic constants using acceptance tested fiber of 10 or more lots.

The specimen selected was a 20-in. diameter bottle based on expediency and cost. The bottle was designed to be wound on a sand mandrel covered with 0.06 in. cured silicone rubber. End closures were wrapped with the baselined 29-deg helical angle fibers, though these end domes were intended for a 25-deg wrap angle. The winding sequence was helical-hoop-helical-hoop-helical for a total thickness of 0.181 in. and stress ratio of helical to hoop of 0.29. Layer thicknesses and properties varied according to the fiber lot used. Bottles were cured and post-cured in a 6 to 1 nitrogen-air environment. The bottles were instrumented with 3 linear variable differential transformers (LVDT) to measure axial displacement and three linear potentiometers (LP) to measure hoop growth. Strain gauges were also applied along the principal axes for comparison.

Manufacturing complication with the compromised mandrel emerged at once. Though the helical angle was only 4 deg in excess of the available 25-deg mandrel, fibers began to slip at the dome ends until the winding operator learned to manually resist the slipping wetted tow. This operator influence was not expected to restore the programmed uniform winding tension on the fiber. The second objection of the sand mandrel was that the expansion of the full scale aluminum mandrel during cure was not being simulated. Both objections were believed to cause slack fibers resulting in low fiber strength and large dispersions. Nevertheless, this series designated as ABA specimen, provided an excellent opportunity to assess instrumentation influences and laminate response verification limitations.

On instrumentation, LVDT proved to be far superior for measuring axial strains consistently and accurately than strain gauges. However, measuring LVDT's was very sensitive to membrane discontinuity stress waves which were noted to propagate over 30 thicknesses from the dome-cylinder intersection. The LP's consistently measure hoop strains about 4 percent low.

Strength and strain dispersions were exorbitantly large though the last 34 bottles, identified as ABA2 series, were an improvement over the first batch because the operator influence improved. Properties and hydrotest data for these ABA2 specimen are documented in Table 6. Later they were abandoned as "A-basis" data, but are included here for scaling trends.

In the meantime, the quarter-scale model case segments were being developed as deliverable articles to verify the FWC dynamics response for on-pad, liftoff, nominal flight, and burnout conditions. The segmented case was 350 in. long with an inside diameter of 36.25 in. measured at the membrane. Metal and composite joints simulated those of the full-scale article and the helical wrap angle was that of the preliminary baseline, ±29 deg.

A number of these segments were scheduled to be hydroproofed to verify the membrane response as well as joint integrity. This test series was identified as DV-36 specimen. To insure that the composite experienced the same thermal exposure as the full scale, a post-cure was imposed on the segment after it was removed from the mandrel to simulate liner vulcanizing environment. It was here discovered that this post-cure caused intolerable radial dimensional changes attributed to stress relief. All subsequent segments were specified to be stress relieved before machining composite ends for joint adapter rings to avoid locked-in discontinuity stresses during liner cure.

Based on the first three hydroburst specimens, it was noted that the average fiber strength increased 10 percent over the ABA2 specimen and was concluded that the DV-36 series was more representative of the manufacturing and cure processes because of the improved mandrel and the increased lamina layers. The "A-basis" allowable test emphasis was switched from the 34 specimen ABA2 series to the 20 specimen DV-36 series. Manufacturing and hydrotest data for 18 specimens are listed in Table 7.

The quarter-scale dynamics test articles were manufactured and hydroproofed before delivery and results are listed in Table 8. Though these eight segments belong to the DV-36 family of specimens, they were characterized separately in this study for comparison.

The laminate baseline was updated at the Critical Design Review. Quarter-scale segments of the deliverable structural test article (STA) were manufactured with the updated laminate system. A variety of structural tests were performed on this quarter-scale series designated as STA Jr. and results from hydrotests are noted in Table 9.

Only three ful-scale test articles have been manufactured and hydrotested. These articles represent the aft segment of the FWC and only the DA003 is of the flight-type composite system. Data reported in Table 10 was considered preliminary at the time of this investigation.

In all the above tables, the fiber volume fraction was calculated from

$$V_f = \frac{(1 - V_d)(1 - W_m)}{(1 - W_m) + W_m \rho_f/\rho_m} \tag{18}$$

where the void fraction was assumed, $V_d = 0.05$, and the resin ratio by weight was controlled at $W_m = 0.327$.

TABLE 6. ABA2 PROPERTIES AND HYDROTEST DATA

Sp. No.	Fiber Lot No.	V_f Percent	V_d Percent	Thicknesses, inch			Load, N_x lb/in.	Percent Strains Measured	
				Helical Layer	Hoop Layer	Total		ϵ_x	ϵ_θ*
1	616-4F	55.8	5.6	0.426	0.0245	0.1768	6279.5	0.1411	0.9838
2	607-3J	54.4	6.5	0.0446	0.0257	0.1852	6276.9	0.1241	0.8469
3	607-3J	54.0	6.1	0.0446	0.0257	0.1852	6276.9	0.1291	0.8635
11	617-4G	53.1	5.1	0.0429	0.0247	0.1781	6279.1	0.1369	0.9595
12	617-4G	56.2	4.6	0.0429	0.0247	0.1781	6279.1	0.1357	0.9882
13	617-4G	53.8	5.1	0.0429	0.0247	0.1781	6279.1	0.1340	0.9772
14	621-3A	52.8	5.7	0.0426	0.0245	0.1768	6279.5	0.1250	0.9540
15	621-3A	56.3	5.6	0.0426	0.0245	0.1768	6279.5	0.1475	0.9750
16	621-3A	51.9	6.2	0.0426	0.0245	0.1768	6279.5	0.1210	0.9374
17	617-4F	52.5	4.2	0.0428	0.0246	0.1776	6279.2	0.1364	1.0286
18	617-4F	53.7	5.1	0.0428	0.0246	0.1776	6279.2	0.1176	0.9419
19	607-3P	53.5	7.3	0.0440	0.0253	0.1826	6277.7	0.1335	0.9143
20	618-3C	53.4	7.4	0.0446	0.0257	0.1852	6276.9	0.1319	0.8767
21	618-3C	56.0	6.3	0.0446	0.0257	0.1852	6276.9	0.1182	0.9209
22	607-3N	53.9	6.7	0.0455	0.0262	0.1889	6275.7	0.1322	0.7947
23	607-3N	52.0	6.7	0.0455	0.0262	0.1889	6275.7	0.1192	0.7847
24	617-4F	54.0	4.3	0.0428	0.0246	0.1776	6279.2	0.1368	0.8667
25	607-3P	53.3	5.7	0.0440	0.0253	0.1826	6277.7	0.1268	0.8893
26	607-3P	52.2	9.5	0.0440	0.0253	0.1826	6277.7	0.1268	0.8775
27	618-3C	52.8	7.8	0.0446	0.0257	0.1852	6276.9	0.1304	0.8480
28	618-3C	53.6	6.1	0.0446	0.0257	0.1852	6276.9	0.1293	0.8500
29	607-3N	54.1	5.8	0.0455	0.0262	0.1889	6275.7	0.1226	0.8499
30	607-3N	53.2	6.9	0.0455	0.0262	0.1889	6275.7	0.1135	0.8555
31	629-3C	56.4	5.9	0.0430	0.0247	0.1784	6279.0	0.1158	0.8400
33	629-3C	57.4	4.2	0.0430	0.0247	0.1784	6279.0	0.1364	0.8864
34	629-3C	59.2	4.9	0.0430	0.0247	0.1784	6279.0	0.1886	0.8201
Mean		54.2	5.98	0.04374	0.02517	0.1815	6277.3	0.1318	0.8973
Percent C.V.		3.2	19.6	2.4	2.4	2.4	0.044	10.7	6.3

3 Layers at +29 deg balanced
3 Layers at - 29 deg Helical
2 Layers at 89.4 deg, Hoop
ρ_m = 0.0437 lb/in.^{3}

Hydro press, P = 1267 psig
H = 0.2773 avg.
E_f = 33.6 MSI, C.V. = 2.1%
I.D. = 20 in.

*Corrected to strain gauge

TABLE 7. DV-36 "A-BASIS" PROPERTIES AND HYDROTEST DATA

SP No.	Fiber Lot No.	V_f Percent	Specimen Thickness, in.				Load N_x lb/in.	Percent Strains Measured	
			Per Layer		Total*	Total			
			Helical	Hoop	Calc.	Meas.		ϵ_x	ϵ_θ
1	607-3I	54.9	0.0491	0.0284	0.2816	0.288	9980.8	0.9577	0.2001
2	607-3I	54.9	0.0491	0.0284	0.2816	0.288	9980.8	0 8756	0.2106
4	619-3A	55.8	0.0505	0.0293	0.2899	0.291	9978.5	0.9244	0.1868
5	617-4G	55.5	0.0477	0.0277	0.2739	0.282	9982.9	1.0169	0.1916
6	630-3A	55.4	0.0472	0.0273	0.2707	0.273	9983.8	1.0033	0.2033
7	629-3C	55.4	0.0477	0.0276	0.2736	0.278	9983.0	0.9777	0.1894
8	617-4G	55.5	0.0477	0.0277	0.2739	0.274	9982.9	1.0166	0.1958
9	629-3C	55.1	0.0476	0.0276	0.2732	0.284	9983.1	0.9776	0.2020
11	619-3A	55.4	0.0505	0.0293	0.2899		9978.5	0.9094	0.1861
12	632-4B	55.2	0.0499	0.0289	0.2803	0.269	9979.5	0.9472	0.1869
13	634-4F	55.3	0.0506	0.0293	0.2903		9978.4	0.9431	0.1874
14	634-4F	55.3	0.0506	0.0293	0.2903		9978.4	1.0160	0.1957
15	629-3C	55.1	0.0477	0.0276	0.2736		9983.0	0.9902	0.1882
16	634-4G	55.4	0.0507	0.0294	0.2910		9978.2	0.9601	0.1979
17	634-4G	55.4	0.0507	0.0294	0.2910		9978.2	0.9603	0.1941
18	630-3A	55.0	0.0472	0.0273	0.2707		9983.8	0.9689	0.1898
19	630-3A	55.0	0.0472	0.0273	0.2707		9983.8	0.9928	0.2023
20	629-3C	55.1	0.0476	0.0276	0.2732		9983.1	0.9725	0.1984
Mean		55.3	0.04885	0.02830	0.2802	0.281	9981.2	0.9672	0.1948
Percent C.V.		0.42	2.90	2.94	2.91	2.6	0.02	3.8	3.5

*Thickness excludes .02 in. glass cloth

ρ_m - 0.0437 for 1 and 2
ρ_m = 0.0444 for 4 through 8
ρ_m = 0.0437 for 9 through 20
3 layers at +29 deg } balanced
3 layers at - 29 deg } helical
2 layers at 90 deg hoop.
1 layer glass cloth 0.02 in. thick
Mean E_{f_L} = 33.78, 1.12 percent C.V.
Hydro press, p = 1110 psig

I D. = 36.25 in.
Calculated effective thickness:
$t_e = t + t_g E_g/E_f = t + 0.0037$ in.
H = 0.3029
Void, V_d = 5 percent

TABLE 8. Q. S. DYNAMICS ARTICLES PROPERTIES

Q.S. Number	Fiber Lot Number	V_f (%)	V_d (%)	Measured Thickness (in.)	Percent Strains Measured	
					ϵ_x	ϵ_θ
1-F	607-3I	61.9	0	0.292	0.1860	0.8300
1-FC	607-3I	61.3	1.0	0.307	0.1743	0.8280
1-AC	607-3I	60.5	0.5	0.293	0.1877	0.8900
1-A	607-3I	56.6	1.6	0.307	0.1927	0.8200
2-F	607-3N	58.0	1.7	0.306	0.1781	0.8500
2-FC	617-4F	55.8	1.6	0.285	0.2052	0.9440
2-AC	7-4F	62.5	0.5	0.279	0.2069	0.9430
2-A	'-4F	60.2	0.8	0.280	0.1458	1.0300
Mean		56.9	0.96	0.294	0.1846	0.8919
Percent C.V.		4.1	61.0	3.8	9.8	7.8

	Helical	Hoop
Angle, deg	±29	90
No. Layers	8	3
Layer Thickness	0.02455	0.0284

Unit load, N_x = 8991 lb/in.

Graphite thickness 0.2816 in.
Glass cloth 0.02 in.
Total thickness 0.3016 in.
I.D. = 36.25 in.
H = 0.3025
Hydrotest pressure, p = 1000 psig

TABLE 9. STA JR. PROPERTIES AND HYDROTEST DATA

SP No. DV-36	Measured Thickness	Hydro Pressure psig	Load N_x lb/in.	Percent Strains Measured	
				ϵ_x	ϵ_θ
-25	0.335	1102	9905.5	0.0650	0.9554
-26		1108	9959.5	0.0400	0.9560
-27		1108	9959.5	0.0424	0.9904
-28		1114	10013.4	0.0441	1.0086
-31		1114	10013.4	0.0442	0.9981
-33		1110	9977.4	0.05612	0.9443
-35		1114	10013.4	0.04322	1.0010
-36		1118	10049.3	0.04838	0.9753
-38		1110	9977.4	0.05548	0.9186
Mean		1110.9	9985.4	0.04882	0.97197
Percent C.V.		4.0	4.0	16.0	2.9

	Helical	Hoop
Fiber Lot No.	640-4B	630-3A
Angle, deg	±33.5	90
No. Layers	12	5
Layer thickness	0.0185	0.0144
Fiber Volume, V_f	55.0%	55.3%

Glass cloth 0.02 in. thick
Voids, V_d = 5 Percent
Total thickness, t = 0.314 in.
H = 0.245
I.D. = 36.25 in.

TABLE 10. FULL-SCALE SEGMENT PROPERTIES AND TEST DATA

Sp. Number	V_f Percent	Thickness* inches		Load N_x lb/in.	Percent Strains Measured	
		Calculated	Measured		ϵ_x	ϵ_θ
DA001	55.2	1.181		32453	0.05144	0.9670
DA002	55.1	1.143		33182	0.05750	0.9850
DA003	58.0	1.308	1.447	37962	0.05043	1.0086

Winding Lay up.	DA001	DA002	DA003
Hoop angle, deg	90	90	90
No. layers	4	4	4
Thickness	0.0312	0.0306	0.03048
No. layers	9	9	11
Thickness	0.0156	0.0153	0.01524
Helical angle, deg	±31.85	±31.85	±33.55
No. layers	28	28	6
Thickness	0.03195	0.0313	0.0156
No. layers			14
Thickness			0.0312
No. layers			6
Thickness			0.052
No. layers			2
Thickness			0.0312
Hoop ratio, H	0.2283	0.2288	0.234
Fiber Lot No.	634-4F -4G	636-4G -4L	
Hydro pressure, psig	901	921	1051

*Includes 0.02 in. graphite cloth
I.D. = 145.23 in.

The axial unit loading experienced by the surface mounted gauges was approximated by

$$N_x = \frac{PR^2}{2R + t} \tag{19}$$

and the thickness of the glass cloth used in quarter-scale specimen was reduced by its stiffness contribution to provide an effective laminate thickness of

$$t = t' + t_g E_g / E_{f_L}$$

where t' is the laminate thickness minus the glass cloth thickness and subscript g refers to glass cloth properties.

As previously mentioned, hydrotests will verify most of the project compliance except the bending-axial stiffness and the diagonal components of A_{ij} and D_{ij} matrices. Equation (5) may be directly verified by uniaxial tests of dog-bone specimens from full-scale articles. One set of such tests has been performed on DA003 membrane,

$$E_x \cdot t = 7.85 \times 10^6 \text{ lbs/in.}$$

More tests are scheduled on this flight-type membrane which will include uniaxial tests in the hoop direction and beam tests on specimen with hoop and axial orientations. Results of these tests will, of course, be used to correlate hydrotest analyses.

VII. LAMINATE VERIFICATION ANALYSIS

If the laminate performance of a flight-type segment has been verified directly by hydrotest and was accepted, why labor over updating the math model? The primary purpose for developing a fine-tuned elastic model was to predict the response for "all" FWC operational loading conditions such as static firing, on-pad cantilevered mode, liftoff and twang transients, ascent flight and reentry through splash-down environments. Included among the loading conditions imposed on the FWC is the acceptance hydroproof test which is comparable to foregoing development hydrotests. If the math model cannot reasonably predict principal strains for a hydroproof test, then there is serious concern that the manned FWC will comply with critical flight environments. It would seem that the bonanza of composite development data represented by Tables 6 through 10 should provide an adequate basis for formulating required laminate math models.

The laminate preliminary stiffness components were forthrightly calculated with estimated average lamina properties, Table 4 and equation (11). Results for the six different development specimens are noted in Table 11. These stiffness components cannot be verified directly but may be backed out from a variety of tests relating stresses and strains. Instrumenting all scheduled hydroproof articles was not only a prudent choice but assured maximum data return. Hydrotests were performed with closed ends so that unit load equations were reduced to

$$N_x = \frac{PR}{2} = \frac{N_\theta}{2}$$

and because both laminate layup and shell geometry are symmetrical, laminate shear is nulled which further reduced constitutive relations of equations (1) to two biaxial strain equations,

$$N_x = A_{11}\,\epsilon_x + A_{12}\,\epsilon_\theta$$

$$2N_x = A_{12}\,\epsilon_x + A_{22}\,\epsilon_\theta \qquad (20)$$

involving three elastic properties. Here was the analytical challenge of the hydrotest program, how to decrease the infinite possible sets of equation (20) solutions to the most likely one.

TABLE 11. ESTIMATED LAMINATE PROPERTIES
(Lamina Modeled from Section V)

Parameters	QS1,2	DV-36	ABA2	DA001,2	STA. Jr	DA003
A_{11} Mppi	2.453	2.439	1.568	9.745	2.347	10.300
A_{22} Mppi	2.119	2.111	1.230	7.452	2.087	8.549
A_{12} Mppi	0.672	0.667	0.438	3.253	0.866	3.898
A_{66} Mppi	0.787	0.783	0.510	3.716	0.987	4.367
D_{11} Kpi	19.97	19.66	5.078	1130.0	19.69	1468.0
D_{22} Kpi	11.75	11.59	2.121	834.0	14.28	1253.0
D_{12} Kpi	5.29	5.21	1.415	365.0	6.96	530.7
D_{66} Kpi	6.12	6.02	1.612	417.0	7.90	603.9
g_1	5.463	5.419	7.621	17.164	10.783	19.639
g_2 Mppi	1.121	1.117	0.640	3.821	1.084	4.372

To start, equations (20) were rewritten to separate laminate stiffness parameter from response parameters, predicted or obtained from hydrotest,

$$g_1 = \frac{\epsilon_\theta}{\epsilon_x} = \frac{2A_{11} - A_{12}}{A_{22} - 2A_{12}}$$

$$g_2 = \frac{N_x}{\epsilon_\theta} = \frac{A_{11}A_{22} - A_{12}^2}{2A_{11} - A_{12}} \qquad (21)$$

The second expression might just as easily be related to the hoop unit load. It turned out that these two ratios conveniently and completely characterized the behavior of a pressurized composite membrane and are here coined as g_n-characteristics or constraints. Calculated stiffness properties, Table 11, were used to predict the g_n-characteristics of equation (21) to compare with those determined from hydrotest data. The approach was adequate for comparing between predictions with an individual test. To derive these characteristics from multiple data of a particular configuration, a curve-fitting method was used with Tables 6 through 9.

It was noted that both expressions in equation (21) are of the form

$$\beta = y_i/x_i$$

and the problem was to calculate the "best fit" y_i and x_i from n-paired observations. Using least square method, β is chosen to minimize

$$\sum_{i=1}^{n} [y_i - \beta x_i]^2$$

Differentiating with respect to β and setting to zero yields the normal equation

$$\beta = \frac{\sum y_i x_i}{\sum x_i^2}$$

or

$$g_1 = \frac{\sum \epsilon_\theta \epsilon_x}{\sum \epsilon_x^2} \quad \text{and} \quad g_2 = \frac{\sum N_x \epsilon_\theta}{\sum \epsilon_\theta^2} \tag{22}$$

Results from hydrotest specimen are listed in Table 12.

Since hydrotest provides the g-characteristics of equations (21), another equation is required to resolve the three stiffness properties of the test article. That equation was formulated [8] from the principle of lease square where the sum of the square of the differences between the observed, A_{ij}, and the estimated, $\hat{A}_{ij}$, parameters results is the smallest possible. This principle is expressed in functional form by

$$f(A_{ij}) = (\hat{A}_{11} - A_{11})^2 + (\hat{A}_{22} - A_{22})^2 + (\hat{A}_{12} - A_{12})^2 = \text{min.} \tag{23}$$

The estimated parameters were derived from preliminary equations (17) whose values are listed in Table 11.

TABLE 12. HYDROTEST DERIVED CHARACTERISTICS
(Tables 6 through 10)

	QS 1,2	DV-36	ABA2	D001,2	STA. Jr.	DA003
No. Bottles	8	18	26	2	9	1
g_1	4.77	4.96	6.77	17.91	19.35	20.0
g_2, Mppi	1.00	1.03	0.696	3.363	1.026	3.764

Using the Lagrange multipliers, λ_n, the functional equation is minimized while satisfying the constraints, g_n, by the expression

$$\frac{\partial f}{\partial A_{ij}} = \frac{\partial}{\partial A_{ij}} [f(A_{ij}) \sum \lambda_n \phi_n] = 0 \quad . \tag{24}$$

Rewriting the constraint equations (21),

$$\begin{aligned} \phi_1 &= 2A_{11} - g_1 A_{22} + A_{12}(2g_1 - 1) = 0 \\ \phi_2 &= 2g_2 A_{11} - A_{11} A_{22} - g_2 A_{12} + A_{12}^2 = 0 \quad , \end{aligned} \tag{25}$$

and substituting with equations (23) into equation (24) gives

$$\begin{aligned} -\sum_{ij} [&(\hat{A}_{11} - A_{11})^2 + (\hat{A}_{22} - A_{22})^2 + (\hat{A}_{12} - A_{12})^2 + \lambda_1(2A_{11} - g_1 A_{22} + A_{12}(2g_1 - 1)) \\ &+ \lambda_2 (2g_2 A_{11} - A_{11} A_{22} - g_2 A_{12} + A_{12}^2)] = 0 \quad . \end{aligned} \tag{26}$$

Making equation (26) stationary with respect to the observed variables, A_{ij},

$$\frac{\partial f}{\partial A_{11}} = -2(\hat{A}_{11} - A_{11}) + 2\lambda_1 + 2\lambda_2 g_2 - \lambda_2 A_{22} = 0$$

$$\frac{\partial f}{\partial A_{22}} = -2(\hat{A}_{22} - A_{22}) - \lambda_1 g_1 - \lambda_2 A_{11} = 0$$

$$\frac{\partial f}{\partial A_{12}} = -2(\hat{A}_{12} - A_{12}) + \lambda_1 (2g_1 - 1) - \lambda_2 g_2 + 2\lambda_2 A_{12} = 0$$

and solving for λ_1 and λ_2 from the first two and substituting into the third gives the desired third equation

$$(1 - 2g_1) A_{11}^2 + [\hat{A}_{11} (2g_1 - 1) - g_1 g_2 - 2\hat{A}_{12}] A_{11} + (2g_1 + 2) A_{11} A_{12}$$

$$- [2g_1 \hat{A}_{11} + 4\hat{A}_{22} + 2g_1 g_2] A_{12} + (4 + g_1) A_{12} A_{22} + [\hat{A}_{22} (1 - 2g_1) \tag{27}$$

$$- 4g_1 g_2 - g_1 \hat{A}_{12}] A_{22} + (2g_1 - 1) A_{22}^2 = - g_1 g_2 [\hat{A}_{11} + 4\hat{A}_{22} + 2\hat{A}_{12}] \quad .$$

The Newton iterative method [9] was used to solve nonlinear algebraic equations simultaneously by expanding in Taylor series about a first approximation and keeping only the first, such as,

$$A_{ij} = A_{ij}^{(1)} + \delta_{ij}^{(1)} \quad , \quad A_{ij}^2 = a_{ij}^{2(1)} + 2a_{ij} \delta_{ij}^{(1)} \quad , \quad \text{etc.}$$

Substituting into equations (25) and (27) and solving for δ_{ij} and then adding these values to the first approximation to yield a second approximation, the procedure is iterated until $\delta_{ij}^{(i)}$ converges. The three simultaneous equations written in final form are

$$2\delta_{11} - g_1 \delta_{22} + (2g_1 - 1) \delta_{12} = -2a_{11} + g_1 a_{22} + (1 - 2g_1) a_{12} \tag{26}$$

$$(2g_2 - a_{22}) \delta_{11} - a_{11} \delta_{22} + (2a_{12} - g_2) \delta_{12} = a_{11} A_{22} - 2g_2 a_{11} + g_2 a_{12} - a_{12}^2 \tag{29}$$

$$[(2g_1 - 1) (\hat{A}_{11} - 2a_{11}) - g_1 g_2 - 2\hat{A}_{12} + 2a_{12} (g_1 + 1)] \delta_{11} + [(2g_1 - 1) (2a_{22} - \hat{A}_{22})$$

$$- 4g_1 g_2 - g_1 \hat{A}_{12} + a_{12} (g_1 + 4)] \delta_{22} + [2a_{11} (g_1 + 1) - 2g_1 \hat{A}_{11} - 4\hat{A}_{22} - 2g_1 g_2$$

$$+ a_{22} (4 + g_1)] \delta_{12} = a_{11}^2 (2g - 1) - a_{11} [\hat{A}_{11} (2g - 1) - g_1 g_2 - 2\hat{A}_{12}]$$

$$- a_{11} a_{22} (2g_1 + 2) + a_{12} (2g_1 \hat{A}_{11} + 4\hat{A}_{22} + 2g_1 g_2) - a_{12} a_{22} (4 + g_1)$$

$$- a_{22} [\hat{A}_{22} (1 - 2g_1) - 4g_1 g_2 - g_1 \hat{A}_{12}] - a_{22}^2 (2g_1 - 1) - g_1 g_2 \hat{A}_{11}$$

$$- 4g_1 g_2 \hat{A}_{22} - 2g_1 g_2 \hat{A}_{12} \tag{30}$$

Equations (28) through (30) are of the form

$$p_1 \delta_{11} + q_1 \delta_{22} + r_1 \delta_{12} = s_1$$

$$p_2 \delta_{11} + q_2 \delta_{22} + r_2 \delta_{12} = s_2$$

$$p_3 \delta_{11} + q_3 \delta_{22} + r_3 \delta_{12} = s_3$$

where δ_{ij} was solved by Cramer's rule through the following expressions

$$U_1 = p_1 (q_2 r_3 - r_2 q_3) - p_2 (q_1 r_3 - r_1 q_3) + p_3 (q_1 r_2 - r_1 q_2)$$

$$U_2 = s_1 (q_2 r_3 - r_2 q_3) - s_2 (q_1 r_3 - r_1 q_3) + s_3 (q_1 r_2 - r_1 q_2) \qquad (31)$$

$$U_3 = p_1 (s_2 r_3 - r_2 s_3) - p_2 (s_2 r_3 - r_1 s_3) + p_3 (s_1 r_2 - r_1 s_2)$$

$$U_4 = p_1 (q_2 s_3 - s_2 q_3) - p_2 (q_2 r_3 - s_1 q_3) + p_3 (q_1 s_2 - s_1 q_2)$$

$$\delta_{11} = U_2/U_1 \quad , \quad \delta_{22} = U_3/U_1 \quad , \quad \delta_{33} = U_4/U_1 \qquad (32)$$

In using the above outlined approach, the "most probable" observed properties for each set of hydrotest articles may be determined if the "estimated" and "observed" are just a few percentages off, otherwise, the estimated modeling should be open to doubt. Table 13 lists the calculated "observed" properties for all six sets of hydrotests and Table 14 provides the comparison in percentage between the estimated and observed, which at a glance was bewildering. Here were over a hundred articles built and tested to the same specifications, but the prediction disparity ranged 40 percent under to 30 percent over. Furthermore, no pattern was discernable as to article size or response dependency. Since the laminate is defined solely by the layup geometries of laminae layers, differences between observed and estimated must be compensated by adjusting the lamina elastic models. That was like dumping another eight unknown variables with only two characteristic equations to resolve them; the observed laminate properties of Table 13 were suspect by the resulting gross disparity; therefore were not counted.

TABLE 13. OBSERVED LAMINATE PROPERTIES
[Equations (25) and (27)]

Laminate Stiffness	QS 1,2	DV-36	ABA2	D001,2	STS. Jr.	DA003
A_{11} Mppi	2.425	2.420	1.570	9.723	2.349	10.273
A_{22} Mppi	1.897	1.951	1.323	6.568	2.005	7.365
A_{12} Mppi	0.492	0.542	0.464	2.820	0.904	3.250

TABLE 14. DEPARTURE OF ESTIMATED FROM OBSERVED PROPERTIES
(Percent)

	QS-1,2	DV-36	ABA2	D001,2	STA. Jr.	DA003
A_{11}	1.1	0.7	0	0.2	- 0.1	0.3
A_{22}	11.7	8.2	- 7.0	13.5	4.1	16.1
A_{12}	36.6	23.2	- 5.6	15.4	- 4.2	18.4
g_1	14.4	9.5	12.5	-4.1	-44.1	-1.8
g_2	12.1	8.4	- 7.5	13.6	5.6	16.2

Surely not all lamina properties were causing g_1 and g_2 characteristic disparity and with some well-grounded judgement, unknown variables may be reduced to a manageable few. To gain this insight, a sensitivity analysis of the g-characteristics with respect to lamina elastic properties was developed. Appendix A.

The sensitivities of the six sets of specimen were noted to vary slightly with geometry but the following generalizations are applicable to all.

The g_2 characteristic is the most difficult to adjust. It is most sensitive to the hoop lamina longitudinal modulus and moderately sensitive (an order of magnitude) to the lamina transverse and inplane shear modulii. It is least sensitive to the helical lamina longitudinal modulus and hoop lamina transverse modulus.

The g_1 characteristic is most sensitive to longitudinal modulii of both helical and hoop lamina. It is one order of magnitude less sensitive to the helical transverse modulus and least sensitive to the hoop lamina transverse modulus.

It appeared that g_2 must be adjusted first by modifying the hoop lamina longitudinal modulus ($\bar{E}_1$) by

$$\bar{E}_1 = 18.6 \left[1 - \frac{\Delta\% \, g_2}{100 \times 18.6 \, (\partial g_2 / \partial \bar{E}_1)} \right] \tag{33}$$

because it is less sensitive to adjustments of g_1 which follows. This was performed for each set of specimen. What resulted was that the g_2 adjustment intensely aggravated the disparity of g_1 characteristic. The new g_1 was adjusted similarly to equation (33). Recalling that g_1 is most sensitive to the longitudinal modulus of the helical lamina, it was modified as noted in Table 15.

In spite of the directness of this approach, a number of serious difficulties turned up that were contrary to experience. While some modification of the in-situ lamina modulii was expected, a 50 percent reduction of the fiber dominated modulus is not conceivable, especially in the hoop lamina – the mechanism is just not there. That one alone was sufficient cause to dismiss this mode of modification and other difficulties became academic.

TABLE 15. LAMINA TRIAL COMPLIANCE WITH TEST g_1 AND g_2

Modified Parameters	QS 1,2	DV	ABA2	DA1,2	STA. Jr.	DA003
g_2 compliance						
Change $\bar{E}_1$, msi	16	17	20	15	17	15
Result g_1 percent	60	53	9	765	-24	-374
g_1 compliance						
Change E_1, percent	16	15	2	61	- 5	- 15
E_1, msi	15.5	15.8	18.2	7.26	19.5	21.5

No doubt the lamina properties must be modified for in-situ conditions, but results must pass the test of experience however limited at this time.

VIII. IN-SITU LAMINA MODELS

In the manufacturing and curing processes, laminate layers experience a wide gradation of polymer changes and imposed contact strains (winding tension, cure and thermal shrinkage, etc.). Intuitively, one might expect the resin connected properties to be especially affected with hoop layers unlike helical ones and thick layers unlike thin ones. Alerted by this possibility and guided by results of Section VII and insights from the sensitivity analysis, the approach for modifying the lamina model to satisfy test data was obvious, first reduce the resin connected modulii as related to manufacturing phenomena and then make up the remaining disparity with fiber connected modulii adjustments.

The first step was crucial to the success of the model and it triggered many collected thoughts and observations of tow winding and resin distribution. In the beginning, the prepared resin is checked for consistency but its tackiness changes with time. The stiffer resin may affect the fiber coating and change the resin-to-fiber ratio and it may also resist compaction and coalescences of adjacent tows. Consequences would be to decrease the lamina modulii and increase the article thickness over that predicted. This occurrence, though ignored, is well known to the industry. But in this investigation it provided a basis for scaling – TIME scaling of the winding process related to resin content and bonding.

Time parameter rightfully belongs in the polymer chemistry domain, nevertheless, it may be roughly related to some available geometric properties of the different set of articles such as

$$E_2, G_{12} \simeq f(N,t,S) \tag{34}$$

where N, t are number of layers and thickness of a laminate and S refers to the scale size of the article.

Another phenomena affecting the resin connected modulii, not time dependent, was realized here. Winding tension on the tow (Fig. 6) is fairly constant for all size articles, wrap angles, and layers. Yet the surface geometry can be shown to vary which has a distinct effect on the tow spread. Assuming the general case of helical winding, the mandrel profile near the tow tangent point may be approximated as an ellipse with R and "b" minor and major semi-axes respectively. The equilibrium equation normal to the tow is

$$N_r\, r\, d\theta - (F + dF) \sin \frac{d\theta}{2} - F \sin \frac{d\theta}{2} = 0$$

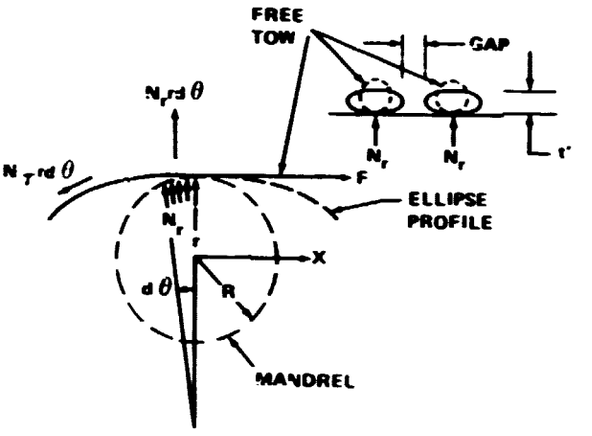

Figure 6. Winding tension effect on tow.

or

$$N_r\, r\, d\theta - F d\theta = 0$$

and
$$N_r = F/r \qquad (35)$$

The physical significance of this expression is that for constant tow tension, the normal unit load acting on the tow is inversely proportional to the radius of curvative "r." Since the ability of the tow to spread (flatten) and touch the adjacent tow is related to the normal load, then the extent of coalescences and voids (gaps) between them is dependent on the radius of curvature at the tow lead-in tangent point (Fig. 6).

The elliptical profile may be better expressed in winding terms such that the major semi-axis is $b = R/\tan \alpha$ where α = helical wind angle. For a hoop wound lamina, $b = R$ so that $\tan \alpha = 1$ and the radius of curvative is identically the madrel radius R and the normal unit load is inversely proportional to the mandrel radius by equation (35). For the helical wound lamina, the radius of curvature is

$$r = [x^2 \tan^4 \alpha + y^2]^{3/2} / R^2 \tan^2 \alpha$$

for $\alpha < 45$ deg. At the point of interest, $x = 0$ and $y = R$ so that the radius of curvature is $r = R/\tan^2 \alpha$ and the normal unit load acting on the helical wound tow is

$$N_r \sim F \frac{\alpha^2}{R}$$

Here another scaling factor was identified, size and helical angle which may relate to the lamina modulii,

$$E_2, G_{12} \sim \alpha^2/S \qquad \text{for} \qquad \alpha < \frac{\pi}{4} \qquad (36)$$

And here again the physical evidence would be an increase in laminate thickness over that predicted but the weight would not increase, voids would.

There exists some evidence that might be attributed to the above phenomena. Seventeen quarter scale specimen (Tables 7 and 8) thicknesses were measured to be 4 percent less than calculated while one full scale (Table 10) shell measured 10 percent thicker than predicted. This is not a sound statistical base for modeling but neither is there a unique method at this time for relating thickness differences to resin elastic degradation nor how to distribute it to gel* and normal load events and to helical and hoop laminae.

One clue for reducing the problem was detected in a fragment from a full scale burst test. The hoop lamina was noted to have a uniformly varying content of resin, and while occasional tows could be identified in most of the acreage, no voids between them were seen. On the other hand, helical tows were densely coated with resin and the gaps between them were noted with few exceptions. Furthermore, helical tows were not completely bonded to the adjacent layers which made it exceedingly easy to peel off each tow at will. These conditions were reported to have degenerated with article size as suggested above.

Another clue was the strain analysis of hoop and helical lamina for resin dependency. The hoop lamina principal strains are coincident with the laminate strains and therefore defined by the g_1 characteristic. For a hoop fiber ultimate strain [equation (7)] of 1.4 percent, the worst case ($g_1 = 4.77$) transverse strain was about 0.3 percent and marginal (Table 3). To determine the helical lamina principal strains, a second order axis transformation was used

$$\begin{Bmatrix} \epsilon_1 \\ \epsilon_2 \\ \frac{\gamma_{12}}{R} \end{Bmatrix} = [T] \begin{Bmatrix} \epsilon_x \\ \epsilon_\theta \\ \frac{\gamma_{x\theta}}{2} \end{Bmatrix}$$

to yield the transverse strain

$$\epsilon_2 = \epsilon_\theta (m^2 + n^2/g_1) \qquad (37)$$

and shear strain

$$\gamma_{12} = 2 \epsilon_\theta mn (1 - 1/g_1) \qquad (38)$$

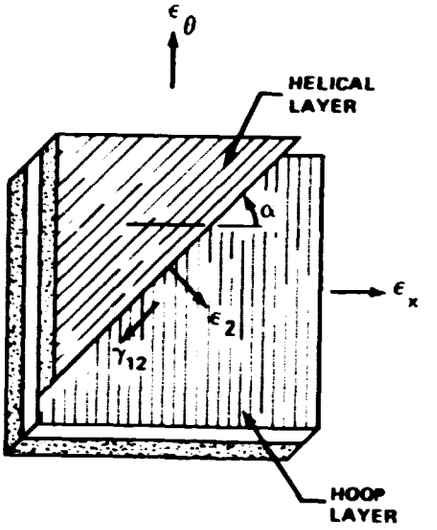

Figure 7. Laminate and lamina strains.

What this analysis implied was that even for large helical angles approaching hoop, the lamina transverse ultimate strain is reached long before the hoop fiber strain capability is achieved (Fig. 7). It does not, however, mean that the transverse modulus is zero. The 4-in. lamina tube only demonstrated that the 3-in. length specimen separated at the weakest link when a strain of 0.293 percent was reached but the remaining length had additional straining capabilities. Recalling how gaps and tow densities (Fig. 6) may vary in a lamina, and particularly the helical lamina, the transverse strain and associated modulus may be

*gel refers to consistency or vitrification.

assumed to act in a loose and variegated pattern across the layer. This is not crazing as many suspected because it is not a uniform separation of fiber from resin within and out the tow.

The full significance of this discussion begins to penetrate when one realizes that here lies the distinction between wound and cloth graphite-epoxy lamina; the wound transverse modulus degenerates to a fraction of the classical, primarily through manufacturing and then through operational strains.

And what about the inplane shear behavior of equation (38). That strain, on the average, is real too but the modulus is variegated like the transverse one. But unlike the transverse modulus, the helical tows may be visualized as a lattice network reaping substantial rigidity from inter-lamina shear between helical and hoop layers. Accordingly, helical lamina shear model should be expected to relate to both g-characteristics.

The final clue was deduced from the sensitivity analysis which clearly indicated that resin connected modulii of the hoop lamina had only third order effects on g_1 and g_2 constraints as determined from the preliminary model. It has even less effects because of the disputed model so why bother revising $\bar{E}_2$, $\bar{G}_{12}$, and $\bar{\nu}_{12}$ models as presented in equations (17)?

Having disposed of insignificant hoop lamina properties, all geometric properties of the six sets of specimen were listed, Table 16, that may be useful to distinguish them in the selection of scaling factors.

TABLE 16. SPECIMEN GEOMETRIC PROPERTIES

Parameter	QS 1,2	DV-36	ABA2	DA01,2	STA. Jr.	DA05
Scale, S	0.25	0.25	0.138	1.0	0.25	1.0
Helical, α	0.506	0.506	0.506	0.556	0.585	0.585
Thickness, t	0.301	0.300	0.181	1.168	0.314	1.308
Layers, N	13	13	8	43	19	49
Hoop, H	0.302	0.303	0.277	0.229	0.245	0.221

Once the environments affecting the transverse modulus of the helical lamina were explained, it was relatively easy to arrive at a reasonable reduction. If the hoop strain is the principal mechanism exercising the helical transverse modulus, then the spacing of helical tow remnants attached along the hoop tows should relate to the proportion of helical lamina engaged. Then the gaps and lack of resin coalescences between helical tows should account for the balance of reduction. Upon review of the fragment from full-scale burst test, tattle-tail epoxy spotting and helical tow scraps on both sides of the hoop lamina were visually estimated at 25 percent. After some manipulations and iterations of parameters, a reasonable prediction of transverse modulus of the helical lamina was empirically obtained,

$$E_2^{\alpha} = 0.27\,\bar{E}_2\,\sqrt[5]{(\alpha^2/NS)} \quad , \tag{39}$$

where $\bar{E}_2$ is the transverse modulus of the hoop lamina and is calculated from equation (17).

Conceding that the transverse modulus had diminished, then the helical lamina major Poisson's ratio must likewise be expected to degrade. In the absence of explicit evidence, and because of its relative insignificance, the helical lamina Poisson's ratio was arbitrarily modeled,

$$\nu_{12}^{\alpha} = 0.53\,\bar{\nu}_{12}\,[\alpha^2/NS]^{0.04} \quad . \tag{40}$$

The helical lamina shear modulus was perhaps the most interesting to modify. It had the property to skew the g-characteristics (reduce one and increase the other simultaneously) and establish a precept to dispersions noted in Table 14. The inplane shear compliance to g-characteristics and parameters in Table 16 was rationalized as follows. The modulus decreases as g_2 decreases and, to a lesser extent (not a continuous lamina), as g_1 increases, was concluded from the sensitivity study. The modulus increases when the interlamina surfaces increase, as discussed above, which may be related to the number of layers (N). However, when the specified layer thickness is small (t/N) and uncontrolled by inadequate compaction, then interlamina contact decreases and shear rigidity decreases. Modulus particularly is reduced with increased scale represented by the thickness. These parameters were cast such that resulting values would allow for reasonable adjustments in longitudinal modulii of hoop and helical lamina when combined into equations (11) and (21) to agree with hydrotest results of Table 12. The final inplane shear modulus of the helical lamina was expressed by

$$G_{12}^{\alpha} = 0.0375\,\bar{G}_{12}\,\frac{g_2}{t\alpha}\,\sqrt{(N/Hg_1)} \tag{41}$$

Having resolved six of the eight lamina elastic constants, there was little latitude left to manipulate the two fiber oriented modulii, hoop and helical. The hoop lamina modulus turned out,

$$E_1^H = 0.089\,\frac{E_1 g_2}{tH}\left[\frac{g_2}{Sg_1}\right]^{0.085} \quad , \tag{42}$$

was dominated by the g_2 characteristic as expected from the sensitivity study and was weakened by the total hoop layer thickness. There was a hint of reduction with increase of g_1 characteristic and scale but it was suspected that this radical would vanish when more full-scale hydrotest and dog-bone data becomes available. A remarkable outcome of this hoop lamina expression was that the longitudinal modulus of the ABA2 and STA Jr. specimen were predicted greater than limit equation (17) and represented by E_1 in equation (42). Both specimens were subscale: ABA2 was smallest and STA Jr. had the most layers of all quarter-scale articles. One explanation may be that the smallest articles allowed for better compaction and the STA Jr. allowed for more compaction opportunities, both leading to reducing the resin content of equation (13). Compaction is applied after each hoop wind with a heavy cloth belt to minimize void.

Finally, the longitudinal modulus of the helical lamina was formulated

$$E_1^{\alpha} = 0.24\,\frac{E_1^H}{S}\,[S^3\,N\,(1.308/t)]^{0.35} \quad , \tag{43}$$

as a function of the hoop lamina longitudinal modulus E_1^H. Scaling with respect to diameter (S) tends to drop out should the radical reconcile to a cube root through a later update. The modulus was inversely responsive to scaling of the thickness (1.308/t).

Curve fit of lamina elastic models with specimen sets are presented in Figure 8, which clearly demonstrates the scaling phenomena (correlation is better than 0.9). Since the slope was sensitive to full-scale articles and since that data is the least available at this time, a later update is incumbent and should incorporate results from scheduled dog-bone specimen tests of full-scale laminate. Curve fits decisively demonstrate scaling dependency of lamina elastic properties. Scaling factors might have been more purely defined if informal test data were not so parsimoniously released by the Prime Contractor. But more to the point is that scaling-up article size decreases lamina stiffness potential. It would seem that a weight decrease of 3 percent or more might be realized through a modest development of tow and resin deployment and control at the winding feed point. The scope is clear.

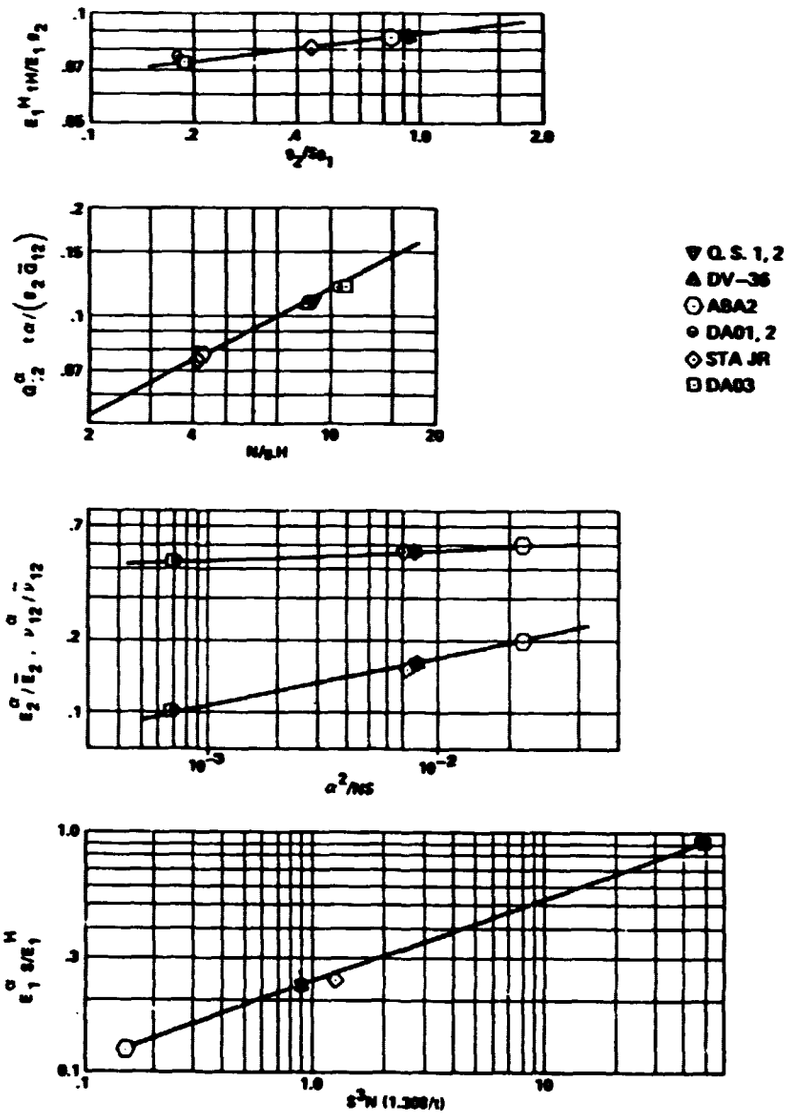

Figure 8. Scaling dependency of lamina elastic constants.

Equations (17) were adjusted by scaling equations (39) through (43) to calculate the lamina constants and laminate stiffness for all the specimen sets and are listed in Table 17. The resulting laminate stiffnesses represent an adjusted set of estimated parameters that were recycled into equations (25) and (27) to obtain a more fitting set of "observed" parameters (Table 18) and as manifested by negligible errors listed in Table 19. Compare these with Table 14.

TABLE 17. ADJUSTED ESTIMATES OF LAMINA AND LAMINATE PROPERTIES

Parameters	QS1,2	DV-36	ABA2	DA1,2	STA. Jr.	DA03
Helical Lamina						
E_1^{α} Msi	16.6	17.3	20.1	17.2	19.7	16.9
E_2^{α} Msi	0.16	0.16	0.20	0.10	0.15	0.10
G_{12}^{α} Msi	0.51	0.52	0.41	0.44	0.30	0.42
ν_{12}^{α}	0.14	0.14	0.15	0.13	0.14	0.13
Hoop Lamina						
E_1^{H} Msi	18	18.4	22.4	18.2	20.1	18
$\bar{E}_2$ Msi	1	1	1	1	1	1
$\bar{G}_{12}$ Msi	0.7	0.7	0.7	0.7	0.7	0.7
$\bar{\nu}_{12}$	0.3	0.3	0.3	0.3	0.3	0.3
A_{ij} Matrix						
$A_{11} \times 10^6$	2.157	2.226	1.63	8.709	2.337	8.994
$A_{22} \times 10^6$	1.902	1.937	1.329	6.540	2.022	7.413
$A_{12} \times 10^6$	0.560	0.579	0.456	2.860	0.913	3.349
$A_{66} \times 10^6$	0.693	0.714	0.526	3.348	1.007	3.876
D_{ij} Matrix	$\times 10^3$	$\times 10^3$	$\times 10^3$	10^6	10^3	10^6
D_{11}	17.66	18.01	5.28	1.014	19.60	1.289
D_{22}	10.24	10.31	2.05	0.733	13.49	1.096
D_{12}	4.42	4.53	1.48	0.321	7.33	0.462
D_{66}	5.38	5.49	1.67	0.376	8.06	0.536

TABLE 18. ADJUSTED OBSERVED LAMINA PROPERTIES

Parameters	Q1,2	DV36	ABA2	DA1.2	STA Jr.	DA03
A_{11}	2.153	2.226	1.630	8.804	2.336	8.992
A_{22}	1.883	1.943	1.325	6.565	2.005	7.362
A_{12}	0.548	0.581	0.455	2.871	0.905	3.314

TABLE 19. DEPARTURE OF SCALED "ESTIMATED" FROM "OBSERVED" PROPERTIES
(Percent)

Parameters	Q1,2	DV36	ABA2	DA1,2	STA Jr.	DA03
A_{11}	0.09	0	0	-1.08	0.04	0.02
A_{22}	0.90	-0.31	0.30	-0.38	0.85	0.69
A_{12}	2.19	-0.34	0.22	-0.38	0.88	1.05

IX. DYNAMICS RESPONSE DILEMMA

Two quarter scale specimen of the type investigated here were dynamically tested and compared with modal predictions using unscaled stiffness matrices. Both shells were vibrated to experimentally determine axial, torsional and shell frequencies. Axial and torsional test results compared favorably with predictions. However, DV and STA Jr. shell frequencies were 15 and 8 percent lower, respectively, than predicted which implied a weakened D_{22} stiffness component as well as a scaling consideration. Differences in laminate bending have been amply published [10,11] and will be investigated for the FWC. However, the lamina properties disparity cause and scaling for static conditions was paramount.

X. CONCLUSIONS

It was inevitable that high performance graphite-epoxy would be counted among space-age materials. Many unexpected singularities have been identified and mastered during the FWC development, such is the wonder of this material, such was the experience with laminate stiffness phenomena.

Graphite-epoxy wound laminate stiffness is unlike its cloth laminate kin in that the epoxy connected lamina properties cannot be fully realized. The mandrel curvature and gel condition of the resin are primary causes affecting the coalescences of tow to adjacent tows and layers to adjacent layers. These conditions were defined as scaling factors related to distinct geometric parameters, though polymer chemists might select more appropriate time factors: they should.

Scaling was amply supported by test evidence, reported observations and curve fits. Having disclosed the phenomena and linking it to stiffness reduction should provide a basis and purpose for winding improvements to realize about three percent weight savings and more efficient structural performance. Ten percent reduction is possible.

In the meantime, serious effort should be directed to translating the "A-basis" ultimate stress (strength) of laminates from quarter-scale specimen to full-scale flight articles with the new baselined system. Results from this investigation provide the insights and rational basis for it.

REFERENCES

1. Ashton, J. and Whitney, J.: Theory of Laminated Plates. Technomic Pub. Co., 1970.

2. Ashton, J., et al.: Primer on Composite Materials: Analysis. Technomic Pub. Co., 1969.

3. Schutz, J.: Final Results of 4-inch Cylinder Test. H1 Memo Misc/6/170-0180, January 18, 1983.

4. Ishikania, T., et al.: Elastic Moduli of Carbon-Epoxy Composites and Carbon Fibers. J. Composite Materials, Vol. II, 1977.

5. Whitney, J. M.: Elastic Moduli of Unidirectional Composites with Anisotropic Filaments. J. Composite Materials, Vol. 1, 1967.

6. Dean, G. and Truner, P.: Elastic Properties of Carbon Fibers and Their Composites. Composites, July 1973.

7. Smith, R. E.: Ultrasonic Elastic Constants of Carbon Fibers and Their Composites. J. Appl. Physics, Vol. 43, June 1972.

8. Verderaime, V. and Rheinfurth, M.: Identification and Management of Filament-Wound Case Stiffness Parameters. NASA Tech Paper 2117, January 1983.

9. Meyer, S. L.: Data Analysis for Scientists and Engineers. John Wiley, 1975.

10. Crawley, E. F.: The Natural Modes of Graphite/Epoxy Cantilever Plates and Shells. J. Composite Materials, Vol. 13, July 1979.

11. Jones, R. M.: Stress-Strain Relations for Materials with Different Moduli in Tension and Compression. AIAA Journal, January 1977.

APPENDIX A

SENSITIVITY ANALYSIS

Sensitivity analysis is a formidable tool in aerospace design to identify and concentrate on the more significant performance variables. Because of the multitude of independent variables that must be satisfied in the design of a high performance filament wound pressure bottle, the author suggested the technique during the FWC feasibility study and imposed it on this contracted project to insure that:

1) Significant independent variables affecting stiffness were identified

2) Stiffness performance dispersions were predicted.

3) A criteria basis was established to specify material acceptance and manufacturing tolerance controls.

During this study, sensitivity analysis again proved its versatility as a diagnostic method for gaining insight into lamina in-situ properties.

Laminate membrane characteristics of interest were defined by

$$g_1 = \frac{2A_{11} - A_{12}}{A_{22} - 2A_{12}}$$

$$G_2 = \frac{A_{11} A_{22} - A_{12}^2}{2A_{11} - A_{12}} \qquad (21)$$

which provide the starting point of this analysis. The variables of concern are the orthotropic elastic properties of the hoop lamina and the helical lamina which are assumed to be different. Using the chain rule of differentiation on the two characteristic equations, the sensitivity coefficient derivations follow.

A) Sensitivity of g-characteristics with respect to laminate properties:

$$dg_1 = b_1\, \partial A_{11} + b_2\, \partial A_{22} + b_3\, \partial A_{12}$$

$$dg_2 = b_4\, \partial A_{11} + b_5\, \partial A_{22} + b_6\, \partial A_{12} \qquad (A\text{-}1)$$

where

$$b_7 = 1/(A_{22} - 2A_{12})$$

$$b_8 = 1/(2A_{11} - A_{12}) \qquad (A\text{-}2)$$

and

$$b_1 = 2b_7 \quad , \quad b_2 = g_1 b_7 \quad , \quad b_3 = (2g_1 - 1)b_7$$

$$b_4 = (A_{22} - 2g_2)b_8 \quad , \quad b_5 = A_{11} b_8 \quad , \quad b_6 = (g_2 - 2A_{12})b_8 \qquad \text{A-3)}$$

B) Laminate Stiffness with respect to lamina variabies:

Using expression (9), the extensional stiffness properties of the laminate may be simplistically formulated from equations (8) and (10) to provide a convenient set of lamina related properties for this analysis. Assuming $E_1/(E_1 - E_2\bar{\nu}_{12}^2) \cong 1$, and designating hoop properties with a bar, then

$$A_{11} = t(1-H)\,[E_1 m^4 + E_2(2\nu_{12} m^2 n^2 + n^4) + 4G_{12} m^2 n^2] + (t\,H\,\bar{E}_2)$$

$$A_{22} = t(1-H)\,[E_1 n^4 + E_2(2\nu_{12} m^2 n^2 + m^4) + 4G_{12} m^2 n^2] + (t\,H\,\bar{E}_1) \qquad \text{(A-4)}$$

$$A_{12} = t(1-H)\,[E_1 m^2 n^2 + E_2(m^2 n^2 + \nu_{12}(m^4 + n^4)) - 4G_{12} m^2 n^2] + (t\,H\,\bar{\nu}_{12}\,\bar{E}_2)$$

and

$$dA_{11} = c_1\,\partial E_1 + c_2\,\partial E_2 + c_3\,\partial \nu_{12} + c_4\,\partial G_{12} + c_5\,\partial \bar{E}_2$$

$$dA_{22} = d_1\,\partial E_1 + d_2\,\partial E_2 + c_3\,\partial \nu_{12} + c_4\,\partial G_{12} + c_5\,\partial \bar{E}_1 \qquad \text{(A-5)}$$

$$dA_{12} = f_1\,\partial E_1 + f_2\,\partial E_2 + f_3\,\partial \nu_{12} + f_4\,\partial G_{12} + f_5\,\partial \bar{E}_2 + f_6\,\partial \bar{\nu}_{12}$$

where

$$c_1 = t(1-H)m^4 \quad , \quad c_2 = t(1-H)(2\nu_{12} m^2 n^2 + n^4)$$

$$c_3 = t(1-H)2E_2 m^2 n^2 \quad , \quad c_4 = t(1-H)(4m^2 n^2) \quad , \quad c_5 = tH$$

$$d_1 = t(1-H)n^4 \quad , \quad d_2 = t(1-H)(2\nu_{12} m^2 n^2 + m^4) \qquad \text{(A-6)}$$

$$f_1 = t(1-H)m^2 n^2 \quad , \quad f_2 = t(1-H)(m^2 n^2 + \nu_{12}(m^4 + n^4))$$

$$f_3 = t(1-H)E_2(m^4 + n^4) \quad , \quad f_4 = -c_4 \quad , \quad f_5 = tH\bar{\nu}_{12} \quad , \quad f_6 = tH\bar{E}_2$$

C) The desired sensitivity coefficients are:

$$\partial g_1/\partial E_1 = b_1c_1 + b_2d_1 + b_3f_1 \qquad \partial g_2/\partial E_1 = b_4c_1 + b_5d_1 + b_6f_1$$

$$\partial g_1/\partial E_2 = b_1c_2 + b_2d_2 + b_3f_2 \qquad \partial g_2/\partial E_2 = b_4c_2 + b_5d_2 + b_6f_2$$

$$\partial g_1/\partial \nu_{12} = b_1c_3 + b_2d_3 + b_3f_3 \qquad \partial g_2/\partial \nu_{12} = b_4c_3 + b_5d_3 + b_6f_3$$

$$\partial g_1/\partial G_{12} = c_4\,(b_1 + b_2 - b_3) \qquad \partial g_2/\partial G_{12} = c_4\,(b_4 + b_5 - b_6) \qquad \text{(A-7)}$$

$$\partial g_1/\partial \bar{E}_1 = b_2\,c_5 \qquad \partial g_2/\partial \bar{E}_1 = b_5\,c_5$$

$$\partial g_1/\partial \bar{E}_2 = b_1\,c_5 + b_3\,f_5 \qquad \partial g_2/\partial \bar{E}_2 = b_4\,c_5 + b_6\,f_5$$

$$\partial g_1/\partial \bar{\nu}_{12} = b_3\,f_6 \qquad \partial g_2/\partial \bar{\nu}_{12} = b_6\,f_6$$

Results for 10 percent change in lamina variables are given by

characteristics, $\Delta\%$ Change = $10\%\ E_i(\partial_{gi}/\partial E_i)/g_i$

laminate , $\Delta\%$ Change = $10\%\ E_i(\partial A_{ij}/\partial E_i)/A_{ij}$ (A-8)

```
REM OS
RUN
INPUT HEL  ANG ,THICKNESS,H-RATIO
29..3016, 3025
```

VARIABLE	NOM VALUE	G1 COEFF	G2 COEFF.	%G FOR 10% VARIABLE G1 CHANGE	G2 CHANGE
HELICAL LAMINA					
E1	1.860E+001	9.331E-001	9.766E-004	3.034E+001	1.588E-001
E2	1.000E+000	2.268E+000	7.900E-002	3.964E+000	6.907E-001
V12	3.000E-001	2.625E+000	3.366E-002	1.377E+000	8.827E-002
G12	7.000E-001	-5.429E-001	9.278E-002	-6.642E-001	5.678E-001
HOOP LAMINA					
E1	1.860E+001	6.883E-001	5.301E-002	2.238E+001	8.620E+000
E2	1.000E+000	6.175E-001	-4.241E-003	1.079E+000	-3.707E-002
V12	3.000E-001	1.256E+000	-5.521E-003	6.587E-001	-1.448E-002
LAMINATE					
A11	2.521E+000	2.637E+000	-2.833E-002	1.162E+001	-6.243E-001
A22	2.165E+000	7.544E+000	5.810E-001	2.855E+001	1.100E+001
A12	7.032E-001	1.377E+001	-6.051E-002	1.692E+001	-3.720E-001

%CHANGE IN Aij per 10% change IN Eij

VARIABLE	A11	A22	A12
HELICAL LAMINA			
E1	9.082E+000	9.985E-001	1.000E+001
E2	1.361E-001	6.735E-001	1.113E+000
V12	9.002E-002	1.048E-001	5.747E-001
G12	4.201E-001	4.892E-001	-1.506E+000
HOOP LAMINA			
E1	0.000E+000	7.839E+000	0.000E+000
E2	3.619E-001	0.000E+000	3.892E-001
V12	0.000E+000	0.000E+000	1.168E-001

```
REM DV
RUN
INPUT HEL. ANG.,THICKNESS,H-RATIO
29,.3001,.3029
```

VARIABLE	NOM. VALUE	G1 COEFF.	G2 COEFF.	%G FOR 10% VARIABLE G1 CHANGE	G2 CHANGE
HELICAL LAMINA					
E1	1.860E+001	9.267E-001	9.726E-004	3.825E+001	1.589E-001
E2	1.000E+000	2.249E+000	7.859E-002	3.947E+000	6.898E-001
V12	3.000E-001	2.604E+000	3.352E-002	1.371E+000	8.825E-002
G12	7.000E-001	-5.361E-001	9.218E-002	-6.586E-001	5.663E-001
HOOP LAMINA					
E1	1.860E+001	6.840E-001	5.282E-002	2.233E+001	8.622E+000
E2	1.000E+000	6.145E-001	-4.224E-003	1.078E+000	-3.708E-002
V12	3.000E-001	1.248E+000	-5.464E-003	6.578E-001	-1.439E-002
LAMINATE					
A11	2.507E+000	2.641E+000	-2.844E-002	1.162E+001	-6.259E-001
A22	2.156E+000	7.525E+000	5.810E-001	2.847E+001	1.099E+001
A12	6.994E-001	1.373E+001	-6.010E-002	1.685E+001	-3.689E-001

%CHANGE IN Aij per 10% change IN Eij

VARIABLE	A11	A22	A12
HELICAL LAMINA			
E1	9.081E+000	9.970E-001	1.000E+001
E2	1.361E-001	6.725E-001	1.113E+000
V12	9.001E-002	1.047E-001	5.747E-001
G12	4.200E-001	4.885E-001	-1.506E+000
HOOP LAMINA			
E1	0.000E+000	7.842E+000	0.000E+000
E2	3.625E-001	0.000E+000	3.899E-001
V12	0.000E+000	0.000E+000	1.170E-001

```
REM ABA
RUN
INPUT HEL. ANG.,THICKNESS,H-RATIO
20.,.181,.2773
```

VARIABLE	NOM. VALUE	G1 COEFF.	G2 COEFF.	%G FOR 10% VARIABLE G1 CHANGE	G2 CHANGE
HELICAL LAMINA					
E1	1.860E+001	1.531E+000	5.547E-004	3.749E+001	1.610E-001
E2	1.000E+000	4.016E+000	4.806E-002	5.289E+000	7.498E-001
V12	3.000E-001	4.633E+000	1.916E-002	1.831E+000	8.970E-002
G12	7.000E-001	-1.221E+000	6.060E-002	-1.126E+000	6.620E-001
HOOP LAMINA					
E1	1.860E+001	1.077E+000	2.916E-002	2.638E+001	8.463E+000
E2	1.000E+000	8.873E-001	-2.358E-003	1.169E+000	-3.679E-002
V12	3.000E-001	2.812E+000	-4.291E-003	7.950E-001	-2.000E-002
LAMINATE					
A11	1.561E+000	5.652E+000	-2.134E-002	1.162E+001	-5.197E-001
A22	1.224E+000	2.146E+001	5.810E-001	3.460E+001	1.110E+001
A12	4.353E-001	4.009E+001	-8.549E-002	2.298E+001	-5.807E-001

%CHANGE IN Aij per 10% change IN Eij

VARIABLE	A11	A22	A12
HELICAL LAMINA			
E1	9.120E+000	1.098E+000	1.005E+001
E2	1.367E-001	7.404E-001	1.118E+000
V12	9.039E-002	1.152E-001	5.773E-001
G12	4.218E-001	5.378E-001	-1.513E+000
HOOP LAMINA			
E1	0.000E+000	7.624E+000	0.000E+000
E2	3.215E-001	0.000E+000	3.459E-001
V12	0.000E+000	0.000E+000	1.038E-001

```
REM DA 1
RUN
INPUT HEL. ANG.,THICKNESS,H-RATIO
31.85,.168,.2288
```

VARIABLE	NOM. VALUE	G1 COEFF.	G2 COEFF.	%G FOR 10% VARIABLE G1 CHANGE	G2 CHANGE
HELICAL LAMINA					
E1	1.860E+001	1.209E+001	5.734E-003	1.105E+002	2.838E-001
E2	1.000E+000	3.257E+001	2.861E-001	1.600E+001	7.614E-001
V12	3.000E-001	3.735E+001	1.202E-001	5.505E+000	9.596E-002
G12	7.000E-001	-1.591E+001	5.551E-001	-5.473E+000	1.034E+000
HOOP LAMINA					
E1	1.860E+001	6.890E+000	1.609E-001	6.296E+001	7.965E+000
E2	1.000E+000	4.709E+000	-1.669E-002	2.314E+000	-4.441E-002
V12	3.000E-001	1.344E+001	-4.669E-002	1.981E+000	-3.727E-002
LAMINATE					
A11	9.675E+000	2.533E+000	-1.004E-002	1.204E+001	-2.584E-001
A22	7.354E+000	2.578E+001	6.021E-001	9.316E+001	1.178E+001
A12	3.282E+000	5.030E+001	-1.747E-001	8.111E+001	-1.526E+000

%CHANGE IN Aij per 10% change IN Eij

VARIABLE	A11	A22	A12
HELICAL LAMINA			
E1	9.016E+000	1.767E+000	1.026E+001
E2	1.844E-001	7.853E-001	1.044E+000
V12	1.122E-001	1.477E-001	4.925E-001
G12	5.238E-001	6.891E-001	-1.544E+000
HOOP LAMINA			
E1	0.000E+000	6.759E+000	0.000E+000
E2	2.762E-001	0.000E+000	2.443E-001
V12	0.000E+000	0.000E+000	7.328E-002

```
REM STA
RUN
INPUT HEL  ANG.,THICKNESS,H-RATIO
33.5,.314,.245
```

VARIABLE	NOM. VALUE	G1 COEFF.	G2 COEFF.	%G FOR 10% VARIABLE G1 CHANGE	%G FOR 10% VARIABLE G2 CHANGE
HELICAL LAMINA					
E1	1.860E+001	5.542E+000	2.200E-003	8.201E+001	3.725E-001
E2	1.000E+000	1.331E+001	7.150E-002	1.059E+001	6.507E-001
V12	3.000E-001	1.536E+001	3.492E-002	3.666E+000	9.535E-002
G12	7.000E-001	-6.200E+000	1.571E-001	-3.453E+000	1.001E+000
HOOP LAMINA					
E1	1.860E+001	3.119E+000	4.743E-002	4.616E+001	8.028E+000
E2	1.000E+000	2.293E+000	-5.672E-003	1.825E+000	-5.161E-002
V12	3.000E-001	5.990E+000	-1.415E-002	1.430E+000	-3.863E-002
LAMINATE					
A11	2.402E+000	6.452E+000	-1.854E-002	1.233E+001	-4.052E-001
A22	2.125E+000	4.054E+001	6.165E-001	6.857E+001	1.192E+001
A12	9.077E-001	7.786E+001	-1.839E-001	5.624E+001	-1.520E+000

%CHANGE IN Aij per 10% chonge IN Eij

VARIABLE	A11	A22	A12
HELICAL LAMINA			
E1	8.877E+000	1.925E+000	1.029E+001
E2	2.171E-001	6.811E-001	1.005E+000
V12	1.255E-001	1.418E-001	4.516E-001
G12	5.854E-001	6.616E-001	-1.549E+000
HOOP LAMINA			
E1	0.000E+000	6.732E+000	0.000E+000
E2	3.203E-001	0.000E+000	2.542E-001
V12	0.000E+000	0.000E+000	7.627E-002

```
REM DA 3
RUN
INPUT HEL. ANG.,THICKNESS,H-RATIO
33.55,1.308,.2214
```

VARIABLE	NOM. VALUE	G1 COEFF.	G2 COEFF.	%G FOR 10% VARIABLE G1 CHANGE	%G FOR 10% VARIABLE G2 CHANGE
HELICAL LAMINA					
E1	1.860E+001	2.607E+001	8.690E-003	1.735E+002	3.795E-001
E2	1.000E+000	6.614E+001	2.982E-001	2.366E+001	7.000E-001
V12	3.000E-001	7.591E+001	1.387E-001	8.147E+000	9.767E-002
G12	7.000E-001	-3.627E+001	7.093E-001	-9.082E+000	1.166E+000
HOOP LAMINA					
E1	1.860E+001	1.362E+001	1.787E-001	9.059E+001	7.804E+000
E2	1.000E+000	8.997E+000	-2.085E-002	3.218E+000	-4.896E-002
V12	3.000E-001	2.674E+001	-6.142E-002	2.870E+000	-4.326E-002
LAMINATE					
A11	1.026E+001	3.364E+000	-8.377E-003	1.234E+001	-2.017E-001
A22	8.379E+000	4.702E+001	6.171E-001	1.409E+002	1.214E+001
A12	3.892E+000	9.235E+001	-2.121E-001	1.286E+002	-1.938E+000

%CHANGE IN Aij per 10% chonge IN Eij

VARIABLE	A11	A22	A12
HELICAL LAMINA			
E1	8.909E+000	2.109E+000	1.032E+001
E2	2.190E-001	7.410E-001	1.007E+000
V12	1.264E-001	1.547E-001	4.519E-001
G12	5.898E-001	7.219E-001	-1.554E+000
HOOP LAMINA			
E1	0.000E+000	6.428E+000	0.000E+000
E2	2.823E-001	0.000E+000	2.232E-001
V12	0.000E+000	0.000E+000	6.696E-002

APPENDIX B

COMPUTER CODES AND RESULTS

- Laminate Stiffness Calculations
- Newton Iterative Method

```
FIND 13
OLD
LIST
100 REM LAMINAT STIFFNESS MATRICES, Aij,Dij
110 SET DEGREES
120 PRINT
130 PRINT "INPUT COMMAND (MATERIALS, LAYERS, OR OUTPUT): ";
140 INPUT C$
150 IF C$="MATERIALS" THEN 180
160 IF C$="LAYERS" THEN 350
170 IF C$="OUTPUT" THEN 490
180 PRINT "INPUT NUMBER OF MATERIAL TYPES: ";
190 INPUT M
200 DELETE E1,E2,E3,E4,E5,C1,C2,C3,C4
210 DIM E1(M),E2(M),E3(M),E4(M),E5(M),C1(M),C2(M),C3(M),C4(M)
220 PRINT "INPUT MAT'L PROP #,E1(J),E2(J),G12(J),U12(J)"
230 INPUT J,X1,X2,X3,X4
240 E1(J)=X1
250 E2(J)=X2
260 E3(J)=X3
270 E4(J)=X4
280 E5(J)=E1(J)/(E1(J)-E2(J)*E4(J)↑2)
290 C1(J)=E1(J)*E5(J)
300 C2(J)=E2(J)*E5(J)
310 C3(J)=E3(J)
320 C4(J)=E4(J)*E2(J)*E5(J)
330 IF J<M THEN 230
340 GO TO 120
350 PRINT "INPUT # OF LAYERS: (0 FOR TAPE INPUT)";
360 INPUT L
365 IF L=0 THEN 5000
370 DELETE T1,B1,M1
380 DIM T1(L),B1(L),M1(L)
400 T0=0
410 PRINT "INPUT LAYER #,MAT'L #, THICKNESS, ANGLE"
420 INPUT I,X1,X2,X3
430 M1(I)=X1
440 T1(I)=X2
450 B1(I)=X3
460 T0=T0+T1(I)
470 IF I<L THEN 420
472 PRINT "STORE DATA ON TAPE? (YES OR NO)"
474 INPUT A$
476 IF A$="YES" THEN 5110
480 GO TO 120
490 DELETE B2,B3,B4,B5,Q1,Q2,Q3,Q4,B6,Q5,Q6
492 DIM B2(L),B3(L),B4(L),B5(L),B6(L)
494 DIM Q1(L),Q2(L),Q3(L),Q4(L),Q5(L),Q6(L)
500 A1=0
510 A2=0
520 A3=0
530 A4=0
540 A5=0
550 A6=0
560 Z1=-T0/2
570 D1=0
580 D2=0
590 D3=0
600 D4=0
610 D5=0
620 D6=0
630 FOR I=1 TO L
640    N=M1(I)
650    B2(I)=COS(B1(I))↑2
660    B3(I)=SIN(B1(I))↑2
670    B4(I)=B2(I)↑2
680    B5(I)=B3(I)↑2
690    B6(I)=COS(B1(I))*SIN(B1(I))
700    Q1(I)=C1(N)*B4(I)+2*(C4(N)+2*C3(N))*B2(I)*B3(I)+C2(N)*B5(I)
710    Q2(I)=C1(N)*B5(I)+2*(C4(N)+2*C3(N))*B2(I)*B3(I)+C2(N)*B4(I)
```

```
720     Q3(I)=(C1(N)+C2(N)-4*C3(N))*B2(I)*B3(I)+C4(N)*(B4(I)+B5(I))
730     Q4(I)=(C1(N)+C2(N)-2*(C3(N)+C4(N)))*B2(I)*B3(I)+C3(N)*(B4(I)+B5(I
        ))
740     Q5(I)=(C1(N)-(C4(N)+2*C3(N)))*B6(I)*B2(I)
750     Q5(I)=Q5(I)+(C4(N)-C2(N)+2*C3(N))*B6(I)*B3(I)
760     Q6(I)=(C1(N)-(C4(N)+2*C3(N)))*B6(I)*B3(I)
770     Q6(I)=Q6(I)+(C4(N)-C2(N)+2*C3(N))*B6(I)*B2(I)
780     A1=A1+Q1(I)*T1(I)
790     A2=A2+Q2(I)*T1(I)
800     A3=A3+Q3(I)*T1(I)
810     A4=A4+Q4(I)*T1(I)
820     A5=A5+Q5(I)*T1(I)
830     A6=A6+Q6(I)*T1(I)
840     Z2=Z1+T1(I)
850     T3=Z2↑3-Z1↑3
860     D1=D1+Q1(I)*T3/3
870     D2=D2+Q2(I)*T3/3
880     D3=D3+Q3(I)*T3/3
890     D4=D4+Q4(I)*T3/3
900     D5=D5+Q5(I)*T3/3
910     D6=D6+Q6(I)*T3/3
920     Z1=Z2
930 NEXT I
940 PRINT "   A MATRIX                                    D MATRIX"
950 IMAGE 3E,1X,3E,1X,3E,2X,3E,1X,3E,1X,3E
960 PRINT USING 950:A1,A3,A5,D1,D3,D5
970 PRINT USING 950:A3,A2,A6,D3,D2,D6
980 PRINT USING 950:A5,A6,A4,D5,D6,D4
990 REM
1000 PRINT "LAMINATE THICKNESS= ";T0
1010 F1=A1*A2-A3↑2
1020 F2=F1/(A2*T0)
1030 F3=F1/(A1*T0)
1040 F4=A3/A2
1050 F5=A4/T0
1060 PRINT "   Ex              Ey              Gxy             Vxy"
1070 IMAGE 3E,3X,3E,3X,3E,3X,3E
1080 PRINT USING 1070:F2,F3,F5,F4
2000 PRINT "COMPARE COMMAND (YES,NO): ";
2010 INPUT D$
2020 IF D$="YES" THEN 2040
2030 IF D$="NO" THEN 120
2040 PRINT "INPUT A11,A22,A12,g1,g2"
2050 INPUT H6,H7,H8,P6,P7
2090 H1=A1*A2-A3↑2
2100 H2=A2-2*A3
2110 H3=2*A1-A3
2120 H4=H3/H2
2130 H5=H1/H3
2200 P1=(A1-H6)*100/H6
2210 P2=(A2-H7)*100/H7
2220 P3=(A3-H8)*100/H8
2230 P4=(H4-P6)*100/P6
2240 P5=(H5-P7)*100/P7
2250 PRINT "PERCENT PREDICTED OVER TEST"
2260 IMAGE 10A,3E
2270 PRINT USING 2260:"A11",P1
2280 PRINT USING 2260:"A22",P2
2290 PRINT USING 2260:"A12",P3
2300 PRINT USING 2260:"g1",P4
2310 PRINT USING 2260:"g2",P5
2320 GO TO 180
4990 REM ** INPUT FROM TAPE **
5000 PRINT "ENTER FILE #"
5010 INPUT F
5020 FIND F
5030 INPUT @33:H$
5040 PRINT H$
5050 INPUT @33:L
5060 DELETE T1,B1,M1
```

```
5070 DIM T1(L),B1(L),M1(L)
5080 INPUT @33:T1,B1,M1
5081 T0=0
5082 FOR K=1 TO L
5084    T0=T0+T1(K)
5086 NEXT K
5090 GO TO 120
5100 REM ** STORE DATA ON TAPE **
5110 PRINT "ENTER HEADER FOR TAPE FILE"
5120 INPUT H$
5130 PRINT "ENTER FILE # TO STORE DATA ON"
5140 INPUT F
5150 FIND F
5160 PRINT @33:H$
5170 PRINT @33:L,T1,B1,M1
5180 GO TO 120
8000 REM FILE 14 : QS1&2  (LAYERS)
8010 REM FILE 15 : DU36A  (LAYERS)
8020 REM  FILE 16:  ABA2   (LAYERS)
8030 REM FILE 17:  DA162  (LAYERS)
8040 REM FILE 18:  STA JR (LAYERS)
8050 REM FILE 19:  DA3    (LAYERS)
```

```
 FIND 13
OLD

RUN

INPUT COMMAND (MATERIALS, LAYERS, OR OUTPUT): MATERIALS
INPUT NUMBER OF MATERIAL TYPES: 3
INPUT MAT'L PROP #,E1(J),E2(J),G12(J),U12(J)
1,18.6,1,.7,.3
2,18.6,1,.7,.3
3,6.6,2,.76,.28

INPUT COMMAND (MATERIALS, LAYERS, OR OUTPUT): LAYERS
INPUT # OF LAYERS: (0 FOR TAPE INPUT)0
ENTER FILE #
14
QSI&2

INPUT COMMAND (MATERIALS, LAYERS, OR OUTPUT): OUTPUT
   A MATRIX                                D MATRIX
 2.453E+000  6.717E-001  0.000E+000   1.997E-002  5.290E-003 -2.690E-004
 6.717E-001  2.119E+000  0.000E+000   5.290E-003  1.175E-002 -9.253E-005
 0.000E+000  0.000E+000  7.876E-001  -2.690E-004 -9.253E-005  6.117E-003
LAMINATE THICKNESS= 0.3016
   Ex              Ey              Gxy             Uxy
 7.427E+000    6.416E+000    2.612E+000    3.170E-001
COMPARE COMMAND (YES,NO): YES
INPUT A11,A22,A12,g1,g2
2.425,1.8969,.4916,4.77,1.0
PERCENT PREDICTED OVER TEST
A11         1.146E+000
A22         1.171E+001
A12         3.663E+001
g1          1.444E+001
g2          1.218E+001
```

```
RUN188
INPUT NUMBER OF MATERIAL TYPES: 3
INPUT MAT'L PROP #,E1(J),E2(J),G12(J),U12(J)
1,16.6,.16,.51,.14
2,18.1,.7,.3
3,6.6,2,.76,.28
   A MATRIX                                D MATRIX
 2.157E+000  5.599E-001  0.000E+000   1.766E-002  4.417E-003 -2.476E-004
 5.599E-001  1.902E+000  0.000E+000   4.417E-003  1.024E-002 -8.857E-005
 0.000E+000  0.000E+000  6.933E-001  -2.476E-004 -8.857E-005  5.380E-003
LAMINATE THICKNESS= 0.3016
   Ex             Ey             Gxy             Uxy
 6.606E+000    5.823E+000    2.299E+000    2.944E-001
PERCENT PREDICTED OVER TEST
A11        -1.104E+001
A22         2.453E-001
A12         1.399E+001
g1          6.816E-001
g2          9.067E-001
INPUT NUMBER OF MATERIAL TYPES:
```

```
FIND13
OLD
RUN

INPUT COMMAND (MATERIALS, LAYERS, OR OUTPUT): MATERIALS
INPUT NUMBER OF MATERIAL TYPES: 3
INPUT MAT'L PROP #,E1(J),E2(J),G12(J),U12(J)
1,18.6,1,.7,.3
2,18.6,1,.7,.3
3,6.6,2,.76,.28

INPUT COMMAND (MATERIALS, LAYERS, OR OUTPUT): LAYERS
INPUT # OF LAYERS: (0 FOR TAPE INPUT)0
ENTER FILE #
15
DV36A

INPUT COMMAND (MATERIALS, LAYERS, OR OUTPUT): OUTPUT
   A MATRIX                                D MATRIX
 2.439E+000  6.677E-001  0.000E+000   1.966E-002  5.205E-003 -2.658E-004
 6.677E-001  2.111E+000  0.000E+000   5.205E-003  1.159E-002 -9.141E-005
 0.000E+000  0.000E+000  7.831E-001  -2.658E-004 -9.141E-005  6.020E-003
LAMINATE THICKNESS= 0.3001
   Ex             Ey             Gxy             Uxy
 7.422E+000    6.424E+000    2.609E+000    3.164E-001
COMPARE COMMAND (YES,NO): YES
INPUT A11,A22,A12,g1,g2
2.420,1.950,.5420,4.96,1.03
PERCENT PREDICTED OVER TEST
A11         7.672E-001
A22         8.240E+000
A12         2.319E+001
g1          9.472E+000
g2          8.429E+000
INPUT NUMBER OF MATERIAL TYPES:
```

```
RUN180
INPUT NUMBER OF MATERIAL TYPES: 2
INPUT MAT'L PROP #,E1(J),E2(J),G12(J),U12(J)
■■■
1,20.1,.2,.41,.15
2,22.4,1,.7,.3
   A MATRIX                                  D MATRIX
 1.631E+000  4.567E-001  3.676E-004   5.285E-003  1.478E-003  4.531E-007
 4.567E-001  1.329E+000  1.093E-002   1.478E-003  2.054E-003  1.347E-005
 3.676E-004  1.093E-002  5.264E-001   4.531E-007  1.347E-005  1.667E-003
LAMINATE THICKNESS= 0.181
   Ex              Ey              Gxy             Uxy
 8.142E+000    6.638E+000    2.908E+000    3.435E-001
PERCENT PREDICTED OVER TEST
A11         3.927E+000
A22         4.801E-001
A12        -1.576E+000
g1         -4.129E-001
g2          3.656E-001
INPUT NUMBER OF MATERIAL TYPES:
```

```
FIND13
OLD
RUN

INPUT COMMAND (MATERIALS, LAYERS, OR OUTPUT): MATERIALS
INPUT NUMBER OF MATERIAL TYPES: 2
INPUT MAT'L PROP #,E1(J),E2(J),G12(J),U12(J)
1,18.6,1,.7,.3
2,18.6,1,.7,.3

INPUT COMMAND (MATERIALS, LAYERS, OR OUTPUT): LAYERS
INPUT # OF LAYERS: (0 FOR TAPE INPUT)0
ENTER FILE #
16
ABA2

INPUT COMMAND (MATERIALS, LAYERS, OR OUTPUT): OUTPUT
   A MATRIX                                  D MATRIX
 1.568E+000  4.378E-001  3.671E-004   5.078E-003  1.415E-003  4.524E-007
 4.378E-001  1.230E+000  8.929E-003   1.415E-003  2.121E-003  1.100E-005
 3.671E-004  8.929E-003  5.099E-001   4.524E-007  1.100E-005  1.612E-003
LAMINATE THICKNESS= 0.181
   Ex              Ey              Gxy             Uxy
 7.804E+000    6.121E+000    2.817E+000    3.559E-001
COMPARE COMMAND (YES,NO): YES
INPUT A11,A22,A12,g1,g2
1.569,1.323,.464,6.77,.696
PERCENT PREDICTED OVER TEST
A11        -4.497E-002
A22        -7.824E+000
A12        -5.645E+000
g1          1.247E+001
g2         -7.502E+000
INPUT NUMBER OF MATERIAL TYPES:
```

```
RUN180
INPUT NUMBER OF MATERIAL TYPES: 3
INPUT MAT'L PROP #,E1(J),E2(J),G12(J),U12(J)
■■■■■■
1,17.3,.16,.52,.14
2,18.4,1,.7,.3
3,6.6,2,.76,.28
   A MATRIX                                  D MATRIX
 2.226E+000  5.798E-001  0.000E+000   1.801E-002  4.526E-003 -2.552E-004
 5.798E-001  1.937E+000  0.000E+000   4.526E-003  1.031E-002 -9.103E-005
 0.000E+000  0.000E+000  7.145E-001  -2.552E-004 -9.103E-005  5.489E-003
LAMINATE THICKNESS= 0.3001
   Ex              Ey              Gxy             Uxy
 6.840E+000    5.953E+000    2.381E+000    2.993E-001
PERCENT PREDICTED OVER TEST
A11         -8.011E+000
A22         -6.475E-001
A12          6.967E+000
g1           3.723E-001
g2          -2.996E-001
INPUT NUMBER OF MATERIAL TYPES:
```

```
FIND 13
OLD
RUN

INPUT COMMAND (MATERIALS, LAYERS, OR OUTPUT): MATERIALS
INPUT NUMBER OF MATERIAL TYPES: 3
INPUT MAT'L PROP #,E1(J),E2(J),G12(J),U12(J)
1,18.6,1,.7,.3
2,18.6,1,.7,.3
3,17.4,1.6,.71,.28

INPUT COMMAND (MATERIALS, LAYERS, OR OUTPUT): LAYERS
INPUT # OF LAYERS: (0 FOR TAPE INPUT)0
ENTER FILE #
19
DA 003   JULY 19 1984

INPUT COMMAND (MATERIALS, LAYERS, OR OUTPUT): OUTPUT
   A MATRIX                                  D MATRIX
 1.030E+001  3.848E+000  0.000E+000   1.468E+000  5.307E-001 -2.848E-002
 3.848E+000  8.549E+000  0.000E+000   5.307E-001  1.253E+000 -1.345E-002
 0.000E+000  0.000E+000  4.367E+000  -2.848E-002 -1.345E-002  6.039E-001
LAMINATE THICKNESS= 1.30796
   Ex              Ey              Gxy             Uxy
 6.550E+000    5.437E+000    3.338E+000    4.501E-001
COMPARE COMMAND (YES,NO): YES
INPUT A11,A22,A12,g1,g2
10.273,7.365,3.250,20,3.764
PERCENT PREDICTED OVER TEST
A11          2.516E-001
A22          1.608E+001
A12          1.840E+001
g1          -1.794E+000
g2           1.617E+001
INPUT NUMBER OF MATERIAL TYPES:
```

```
RUN180
INPUT NUMBER OF MATERIAL TYPES: 3
INPUT MAT'L PROP #,E1(J),E2(J),G12(J),U12(J)
1,16.9,.1,.42,.13
2,18,1,.7,.3
3,17.4,1.6,.71,.28
   A MATRIX                                  D MATRIX
 8.994E+000  3.349E+000  0.000E+000   1.289E+000  4.623E-001 -2.698E-002
 3.349E+000  7.413E+000  0.000E+000   4.623E-001  1.096E+000 -1.286E-002
 0.000E+000  0.000E+000  3.876E+000  -2.698E-002 -1.286E-002  5.366E-001
LAMINATE THICKNESS= 1.30796
   Ex                Ey                Gxy               Uxy
 5.719E+000    4.714E+000    2.963E+000    4.518E-001
PERCENT PREDICTED OVER TEST
A11        -1.245E+001
A22         6.577E-001
A12         3.047E+000
g1          2.313E+000
g2          6.523E-001
INPUT NUMBER OF MATERIAL TYPES:
```

```
FIND13
OLD
RUN

INPUT COMMAND (MATERIALS, LAYERS, OR OUTPUT): MATERIALS
INPUT NUMBER OF MATERIAL TYPES: 3
INPUT MAT'L PROP #,E1(J),E2(J),G12(J),U12(J)
1,18.6,1,.7,.3
2,18.6,1,.7,.3
3,6.6,2,.76,.28

INPUT COMMAND (MATERIALS, LAYERS, OR OUTPUT): LAYERS
INPUT # OF LAYERS: (0 FOR TAPE INPUT)0
ENTER FILE #
18
STA JR

INPUT COMMAND (MATERIALS, LAYERS, OR OUTPUT): OUTPUT
   A MATRIX                                  D MATRIX
 2.347E+000  8.663E-001  0.000E+000   1.969E-002  6.964E-003 -2.273E-004
 8.663E-001  2.087E+000  0.000E+000   6.964E-003  1.428E-002 -1.070E-004
 0.000E+000  0.000E+000  9.072E-001  -2.273E-004 -1.070E-004  7.900E-003
LAMINATE THICKNESS= 0.314
   Ex                Ey                Gxy               Uxy
 6.331E+000    5.628E+000    3.144E+000    4.151E-001
COMPARE COMMAND (YES,NO): YES
INPUT A11,A22,A12,g1,g2
2.349,2.805,.9045,19.35,1.026
PERCENT PREDICTED OVER TEST
A11        -6.441E-002
A22         4.078E+000
A12        -4.226E+000
g1         -4.414E+001
g2          5.600E+000
INPUT NUMBER OF MATERIAL TYPES:
```

```
RUN180
INPUT NUMBER OF MATERIAL TYPES: 3
INPUT MAT'L PROP #,E1(J),E2(J),G12(J),U12(J)
1,19.7,.15,.30,.14
2,20.1,1,.7,.3
3,6.6,2,.76,.28
   A MATRIX                                  D MATRIX
 2.337E+000  9.130E-001  0.000E+000   1.960E-002  7.334E-003 -2.535E-004
 9.130E-001  2.022E+000  0.000E+000   7.334E-003  1.349E-002 -1.161E-004
 0.000E+000  0.000E+000  1.007E+000  -2.535E-004 -1.161E-004  8.060E-003
LAMINATE THICKNESS= 0.314
   Ex             Ey             Gxy             Uxy
 6.130E+000     5.304E+000     3.203E+690     4.515E-001
PERCENT PREDICTED OVER TEST
A11         -5.145E-001
A22          8.596E-001
A12          9.448E-001
g1          -9.116E-001
g2           8.701E-001
INPUT NUMBER OF MATERIAL TYPES:
```

```
FIND13
OLD
RUN

INPUT COMMAND (MATERIALS, LAYERS, OR OUTPUT): MATERIALS
INPUT NUMBER OF MATERIAL TYPES: 3
INPUT MAT'L PROP #,E1(J),E2(J),G12(J),U12(J)
1,18.6,1,.7,.3
2,18.6,1,.7,.3
3,17.4,1.6,.71,.28

INPUT COMMAND (MATERIALS, LAYERS, OR OUTPUT): LAYERS
INPUT # OF LAYERS: (0 FOR TAPE INPUT)0
ENTER FILE #
17
DA 1&2

INPUT COMMAND (MATERIALS, LAYERS, OR OUTPUT): OUTPUT
   A MATRIX                                  D MATRIX
 9.745E+000  3.253E+000  0.000E+000   1.130E+000  3.650E-001 -4.667E-003
 3.253E+000  7.452E+000  0.000E+000   3.650E-001  8.339E-001 -1.961E-003
 0.000E+000  0.000E+000  3.716E+000  -4.667E-003 -1.961E-003  4.170E-001
LAMINATE THICKNESS= 1.16801
   Ex             Ey             Gxy             Uxy
 7.127E+000     5.450E+000     3.182E+000     4.366E-001
COMPARE COMMAND (YES,NO): YES
INPUT A11,A22,A12,g1,g2
9.723,6.568,2.820,17.91,3.363
PERCENT PREDICTED OVER TEST
A11          2.224E-001
A22          1.346E+001
A12          1.537E+001
g1          -4.115E+000
g2           1.361E+001
INPUT NUMBER OF MATERIAL TYPES:
```

```
RUN100
INPUT NUMBER OF MATERIAL TYPES: 3
INPUT MATERIAL PROP #,E1(J),E2(J),G12(J),U12(J)
1,17.2,.10,.44,.13
2,18.2,1,.7,.3
3,17.4,1.6,.71,.28
   A MATRIX                                  D MATRIX
 8.709E+000  2.860E+000  0.000E+000   1.014E+000  3.219E-001 -4.493E-003
 2.860E+000  6.540E+000  0.000E+000   3.210E-001  7.328E-001 -1.916E-003
 0.000E+000  0.000E+000  3.348E+000  -4.493E-003 -1.916E-003  3.758E-001
LAMINATE THICKNESS= 1.16801
   Ex              Ey              Gxy             Uxy
 6.385E+000    4.795E+000    2.966E+000    4.373E-001
PERCENT PREDICTED OVER TEST
A11        -1.043E+001
A22        -4.245E-001
A12         1.411E+000
g1         -9.424E-001
g2         -3.670E-001
INPUT NUMBER OF MATERIAL TYPES:
```

```
FIND 6
OLD
LIST
7 FIND 6
100 REM LAMINATE HYDROTEST PROPERTIES, NEWTON ITERATIVE METHOD
110 REM PREDICTED:B1=A11,B2=A22,B3=A12. TEST:B5=g1,B6=g2
120 REM DETEPMINE:A1=A11* ,A2=A22* ,A3=A12*
200 PRINT "INPUT PRED.A11,A22,A12. TEST g1, g2 "
210 INPUT B1,B2,B3,B4,B5
230 PRINT "INPUT TRIAL a11,a22,a12"
240 INPUT B7,B8,B9
250 PRINT "INPUT NUMBER OF ITERATIONS "
251 INPUT K
260 I=0
300 L1=2
310 M1=-B4
320 N1=2*B4-1
330 C1=-2*B7+B4*B8-(2*B4-1)*B9
350 L2=2*B5-B8
360 M2=-B7
370 N2=2*B9-B5
380 C2=-2*B5*B7+B7*B8+B5*B9-B9↑2
400 L3=-2*B7*(2*B4-1)+B1*(2*B4-1)-2*B3-B4*B5+B9*(2*B4+2)
410 M3=B9*(B4+4)-B4*B3-B2*(2*B4-1)-4*B4*B5+2*B8*(2*B4-1)
420 N3=-2*B4*B1-2*B4*B5-4*B2+B8*(B4+4)+B7*2*(B4+1)
430 C3=(2*B4-1)*B7↑2-B7*(B1*(2*B4-1)-2*B3-B4*B5)-2*(B4+1)*B7*B9
440 C3=C3+B9*(2*B4*B1+2*B4*B5+4*B2)-B9*B8*(B4+4)+B8*(B4*B3+B2*(2*B4-1))
450 C3=C3+B8*4*B4*B5-(2*B4-1)*B8↑2-B4*B5*(B1+2*B3+4*B2)
500 D1=L1*(M2*N3-M2*M3)-L2*(M1*N3-N1*M3)+L3*(M1*N2-N1*M2)
510 D2=C1*(M2*N3-N2*M3)-C2*(M1*N3-N1*M3)+C3*(M1*N2-N1*M2)
520 D3=L1*(C2*N3-N2*C3)-L2*(C1*N3-N1*C3)+L3*(C1*N2-N1*C2)
530 D4=L1*(M2*C3-C2*M3)-L2*(M1*C3-C1*M3)+L3*(M1*C2-C1*M2)
540 X=D2/D1
550 Y=D3/D1
560 Z=D4/D1
570 PRINT "X,Y,Z. ";X,Y,Z
600 B7=B7+X
610 B8=B8+Y
620 B9=B9+Z
630 PRINT "TEST A11, A22, A12 ";B7,B8,B9
640 I=I+1
650 IF I<K THEN 300
660 END
```